

Salvorin is the allosteric drug studied here with orthosteric DAMGO bound and apo protein

# Activation and Allosteric Modulation of Human $\mu$ Opioid Receptor in Molecular Dynamics

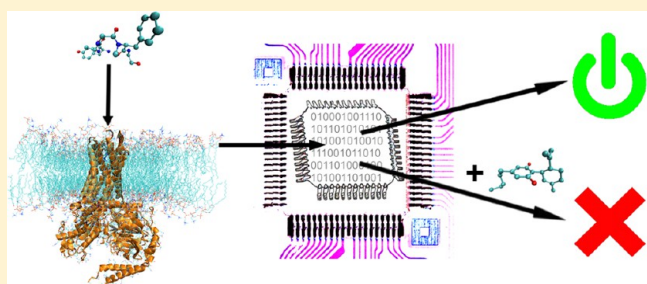
Damian Bartuzi,\*† Agnieszka A. Kaczor,‡,§ and Dariusz Matosiuk†

†Department of Synthesis and Chemical Technology of Pharmaceutical Substances with Computer Modeling Lab, Faculty of Pharmacy with Division of Medical Analytics, Medical University of Lublin, 4A Chodźki St., PL-20093 Lublin, Poland

‡School of Pharmacy, University of Eastern Finland, Yliopistonranta 1, P.O. Box 1627, FI-70211 Kuopio, Finland

## Supporting Information

**ABSTRACT:** Allosteric protein modulation has gained increasing attention in drug design. Its application as a mechanism of action could bring forth safer and more effective medicines. Targeting opioid receptors with allosteric modulators can result in better treatment of pain, depression, and respiratory and immune disorders. In this work we use recent reports on negative modulators of  $\mu$  opioid receptor as a starting point for identification of allosteric sites and mechanisms of opioid receptor modulation using homology modeling and docking and molecular dynamics studies. An allosteric binding site description is presented. Results suggest a shared binding region for lipophilic allosteric ligands, reveal possible differences in the modulation mechanism between cannabinoids and salvinorin A, and show ambiguous properties of the latter. Also, they emphasize the importance of native-like environment in molecular dynamics simulations and uncover relationships between modulator and orthosteric ligand binding and receptor behavior. Relationships between ligands, transmission switch, and hydrophobic lock are analyzed.



## INTRODUCTION

In recent years, one can observe a turn in drug design toward subtle and sophisticated mechanisms with a potential for precise protein regulation, even on the level of specific signaling pathways.<sup>1</sup> This is also the case for G protein-coupled receptors (GPCRs). Biased signaling, receptor homo- and heterodimerization with the possibility of targeting particular dimers with drugs, as well as allosteric modulation gain nowadays increasing attention as a potential source of safer and more effective drugs. Allosteric modulators can bias a receptor to act through the desired pathway upon ligand binding and can modulate dimer formation.<sup>2</sup> Benefits of this mode of action cannot be overemphasized: allosteric modulators could allow for both spatial and temporal selectivity—they preserve physiological patterns of activation/deactivation, augmenting or silencing effects of endogenous ligand. Thanks to dependence of activation on concentration of the latter, response to modulator is subordinated to physiological regulatory mechanisms, and therefore the potential of overdose is decreased. Moreover, smaller evolutionary pressure on structure preservation of allosteric binding sites compared to orthosteric ones results in a greater structural divergence of these sites, which facilitates achieving selectivity. Modulators offer even more possibilities, e.g. probe dependence—a property making a modulator affect only a specific ligand without any effect on other ligands of the same protein.

GPCRs are a particularly interesting group of drug targets that could be addressed by potential allosteric modulators.<sup>3</sup>

Currently GPCRs are intensively investigated in the pharmaceutical industry as they constitute targets for about 50% of recently launched drugs.<sup>4</sup> These receptors are the largest family of membrane proteins and mediate most cellular responses to various stimuli—endogenous, like hormones and neurotransmitters, as well as exogenous: photons, olfactory, and taste impulses.

Opioid receptors (ORs) are assigned by the GRAFS<sup>5</sup> and the “A–F”<sup>6</sup> GPCR classification systems to the rhodopsin family, which is the largest and the most diverse of all GPCR families. The family is further divided into subfamilies following different evolutionary pathways,<sup>7</sup> with ORs belonging to the G1 group, together with purinergic, chemotactic, and somatostatin receptors. Consequences of this classification are important e.g. for homology modeling of G1-belonging receptors and for considering appliance of general GPCR activation patterns.

ORs are a molecular target for a number of approved drugs, ranging from powerful antinociceptive agents (e.g., fentanyl) to freely accessible antitussive medicines (codeine). They are involved in nociception, respiratory, digestive, and immune system control, mood regulation, and affect reward mechanisms. Unfortunately, abundance of these receptors in various systems, high homology, and particularly the connection with the reward system result in serious side effects and high addictive potential of their ligands, dramatically restricting

Received: February 13, 2015

Published: October 30, 2015

overall purpose  
yuan paper is referred here in an intro reference goal

applications of this class of drugs. The increase in receptor subtype-specificity may not be sufficient to overcome the impasse, since most of both desired and undesired effects are involved in  $\mu$  opioid receptor (MOR) activation. New possibilities appear with GPCR allosteric modulators. The modulation could make it possible to isolate desired activity from side effects. The approval of the first two allosteric drugs targeting GPCRs, Cinacalcet (2005) and Maraviroc (2007), proves the usefulness of this class of drugs.

Limitations in experimental examination of allostery make computer aided drug design (CADD) techniques the methods of choice. Molecular dynamics (MD) has been recently employed to explain the effect of sodium ions on MOR,<sup>8,9</sup> relationship between water chain formation inside the GPCR 7TM bundle and the receptor activation<sup>10</sup> as well as interaction of muscarinic M<sub>2</sub> receptor and its allosteric modulator. Yet, investigation of sodium ion influence<sup>8,9</sup> remains the only MD simulation of an allosteric modulator acting at rhodopsin G1 subfamily receptor. A small number of simulations regarding GPCR allosteric modulation have appeared so far, predominantly concerning M<sub>2</sub> muscarinic acetylcholine receptor modulation.<sup>11,12</sup>

Although CADD methods have been recently applied to MOR, mostly the mouse MOR X-ray structure (PDB ID: 4DKL<sup>13</sup>) was used for simulations. Also, predominantly rigid compounds were employed as orthosteric ligands, with few exceptions.<sup>14</sup> The 4DKL structure reflects MOR inactive conformation, where the 7TM bundle is densely packed and residues responsible for interactions of the G protein with the MOR interior are hidden. The data obtained by Provasi et al. indicate that presence of a G protein or its mimetic is important in simulations.<sup>15</sup> Moreover, as MOR native ligands are peptides and allosteric modulation is probe-dependent, an insight into flexible ligand-MOR interactions would be beneficial for understanding of 7TM peptide receptors.

On the other hand, there is an increase in OR allosteric modulators identified. Negative—tetrahydrocannabinol (THC), cannabidiol (CDI),<sup>16</sup> and salvinorin A<sup>17</sup>—and recently also positive—BMS-986121 and BMS-986122<sup>18</sup> allosteric modulators have been reported. This enables identification of an allosteric pocket and performing a detailed analysis of OR modulation mechanisms.

CADD methods produce wealth of data, yet often sifting essential information from noise is problematic. To solve this problem, principal component analysis (PCA) can be used.<sup>19</sup> The procedure facilitates recognition of relevant motions. It was successfully applied also to GPCR MD analysis.<sup>20,21</sup>

In this study, allosteric modulation of MOR was analyzed with computational methods based on experimental data. In particular, a series of all-atom MD simulations was performed and subsequently analyzed with PCA. The performed analysis aims to identify a binding pocket, describe key MOR interactions with negative allosteric modulators, as well as to investigate underlying modulation mechanisms.

## EXPERIMENTAL SECTION

**Homology Modeling.** Homology modeling was performed as previously described.<sup>22</sup> In summary, MAFFT<sup>23</sup> was used for multisequence alignment of human family A GPCRs excluding olfactory receptors. Sequences were obtained from the UniProt database and aligned with the BLOSUM 30 scoring matrix for identification of the regions of key importance, and subsequently, the target and a set of templates were extracted

and manually refined. Additional alignment of templates and target only with the BLOSUM 62 scoring matrix was used for validation. The templates used were: mouse MOR (PDB ID: 4DKL<sup>13</sup>), turkey  $\beta_1$  adrenergic receptor (PDB IDs: 2Y00, 2Y01, 2Y02, 2Y03, 2Y04<sup>24</sup>), human  $\beta_2$  adrenergic receptor (PDB IDs: 3POG, 3PDS, 3SN6<sup>25–27</sup>), and human A<sub>2A</sub> adenosine receptor (PDB IDs: 2YDO, 2YDV, 3QAK<sup>28,29</sup>). Five populations of 100 models each based on different combinations of templates were created with Modeler v. 9.10.<sup>30</sup> Model selection was based on docking, scoring functions and experimental data. The model for further investigation was chosen as described in the **Results and Discussion** section and belongs to the fifth population (referred to as population E in the original modeling paper<sup>22</sup>) constructed on the basis of fully activated-state templates 3SN6 and 3POG and an inactive 4DKL structure without its TM VI helix. This model consists of a 7TM MOR domain with an N-terminal cut at Thr 61 and C-terminal cut at Pro 355, and G<sub>s</sub> protein complex. We decided to model the MOR-G<sub>s</sub> complex, since although less known, MOR-G<sub>s</sub> coupling is proven to occur,<sup>31</sup> and it allowed for a more reliable modeling of the protein–protein interface. In particular, active state 3SN6 and 3POG structures served as only templates for modeling of intracellular part of TM VI, while the use of 4DKL structure allowed for proper modeling of TM II in the region of Pro 2.58, which is a region distinguishing G1 subfamily from other rhodopsin receptor subfamilies, including G2 belonging 3SN6 and 3POG active-state templates.

**Ligand Preparation.** Ligands were downloaded from the Cambridge Structural Database (CSD; morphine, salvinorin A, cannabidiol)<sup>32</sup> or built and refined with the Spartan10 software<sup>33</sup> ([D-Ala<sup>2</sup>, N-MePhe<sup>4</sup>, Gly-ol]-enkephalin [DAMGO], THC, herkinorin). The conformers were chosen after equilibrium conformer search with the molecular mechanics empirical scheme (MMFF), followed by geometry optimization employing density functional theory (B3LYP) using the 6-31G\* basis set.

**Molecular Docking.** Molecular docking of negative modulators to previously published MOR homology model<sup>22</sup> was performed with Surflex module of the SybylX 1.3.<sup>34</sup> The docking destination was initially set to extracellular part of the receptor, and subsequently restrained to identified binding sites for pose refinement. Docking results were assessed based on available experimental data as well as scoring function results and visual inspection. Several docking poses of all ligands were selected and the final pose of each ligand was chosen based on its best stability after initial 20 ns simulations (Figure S3). For salvinorin A agreement with experimental data was a decisive factor.

**Molecular Dynamics (MD).** The construction of simulation boxes was performed as follows: homology models were immersed in a pure 1-palmitoyl-2-oleoyl-sn-glycero-3-phosphocholine (POPC) membrane, POPC with 20% cholesterol (CHL), POPC with 40% CHL, or in a native-like raft membrane, composed of 30% CHL, 20% sphingomyelin (SM), 25% POPC, and 25% 1-palmitoyl-2-oleoyl-sn-glycero-3-phosphoethanolamine (POPE);<sup>35</sup> then, the box was filled with water and ions (0.15 M NaCl). Force fields used for system description were the following: Amber03 force field<sup>36</sup> for protein, GAFF<sup>37,38</sup> for ligands, Stockholm lipids<sup>39–41</sup> for membrane. The TIP3P water model was used. Ligand topologies were obtained with RESP ESP charge Derive Server (REDS)<sup>42</sup> and Acyppe.<sup>43</sup> Membranes were constructed with CHARMM Membrane Builder<sup>44</sup> and modified with a SybylX

1.3 script to introduce sphingomyelin. Membrane–protein complexes were subjected to steepest descent minimization (a simple gradient method and a first order minimizer; it uses the first derivative of the potential energy with respect to the Cartesian coordinates; the method moves down the steepest slope of the interatomic forces on the potential energy surface; the descent is accomplished by adding an increment to the coordinates in the direction of the negative gradient of the potential energy, or the force) and equilibrated by 1 ns NVT and 50 ns NPT with protein restrained by a force constant of 10 000 kJ/mol nm<sup>2</sup>, with use of GROMACS 4.6.<sup>45</sup> Next, the protein was replaced with protein–ligand complexes or the protein apo form, colliding water molecules, and a sodium ion migrating to Asp 2.50 were removed. Systems were minimized by steepest descent and equilibrated by 1 ns NVT and 20 ns NPT with protein and ligands restrained by force constant of 1000 kJ/mol nm<sup>2</sup>. In order to choose the most favorable modulator positions nine 20 ns-long simulations were performed (Figure S3). Unrestrained production runs were performed for 100 ns for each system. There were 25 simulations of the chosen model and ligand poses performed. This made the total of 2.5  $\mu$ s of production run (Table 1).

**Table 1. Numbering of MOR Systems for the MD Simulations<sup>a</sup>**

	raftlike	POPC	POPC + 20% cholesterol	POPC + 40% cholesterol
apo-MOR	11	12	13	14
MOR + morphine	21	22	23	24
MOR + DAMGO	31	32	33	34
MOR + herkinorin	41			
MOR + salvinorin A	51	52	53	54
MOR + THC	61			
MOR + cannabidiol	71			
MOR + DAMGO + salvinorin A	81	82	83	84
MOR + DAMGO + THC	91			
MOR + DAMGO + cannabidiol	101			

<sup>a</sup>The systems are referred by double- or triple-digit numbers. The first digit (or the first two digits for the last row) indicates ligands configuration, and the last digit indicates membrane environment.

Nose-Hoover thermostat and Parrinello–Rahman pressure coupling at the NPT step was used in equilibration as well as in production MD. Timestep of 2 fs was used. Data were collected every 50 ps.

**Results Analysis and Presentation.** Extraction of the data from result files and most of the analysis was done with standard GROMACS tools. Preparation of graphs and analysis of data matrices were performed with MS Excel and OpenOffice.org, as well as the R software.<sup>46</sup> Figures were prepared with VMD 1.9.1<sup>47</sup> or PyMOL 1.5.0.4.<sup>48</sup>

## RESULTS AND DISCUSSION

**Molecular Docking.** The careful choice of docking results was crucial for potentially successful identification of the allosteric binding site. For salvinorin A, a neoclerodane diterpene, there is available site-directed mutagenesis data.<sup>49</sup> In particular Ile 316 (7.39 according to the Ballestros–Weinstein nomenclature<sup>50</sup>), Tyr 320 (7.43), Gln 115 (2.60), Tyr 312 (7.35), Tyr 313 (7.36), and Tyr 119 (2.64) in  $\kappa$  opioid receptor

(KOR) are proposed to participate in salvinorin-mediated activation. Moreover, selectivity of salvinorin A toward the activation of KOR, versus herkinorin (2-benzoyl-salvinorin) being selective to MOR provides additional information. Salvinorin A is a potent KOR agonist with nanomolar affinity. It also acts on MOR as a weak negative allosteric agent with micromolar affinity. Since sequence identity between these two proteins is considerable (56.44% for entire sequences) and high-resolution X-ray structures of both receptors are available,<sup>13,51</sup> the superposition of these structures can be informative (Figure 1). There are differences in the putative

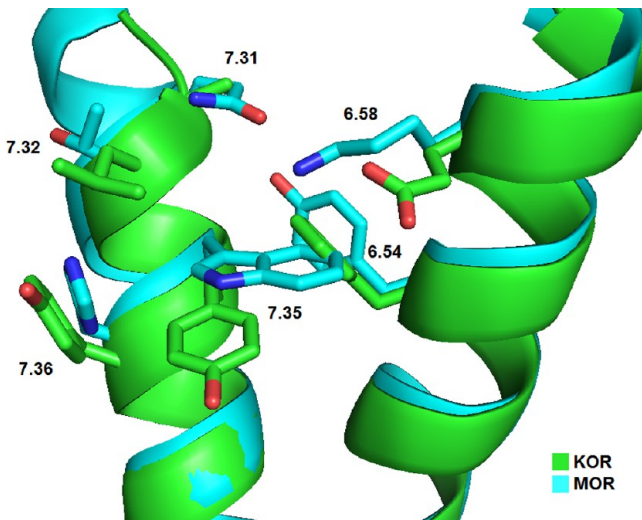


**Figure 1.** Superposition of TM VI and TM VII of MOR (PDB ID: 4DKL) and KOR (PDB ID: 4DJH) with marked most significant differences. Hydrogen atoms omitted for clarity.

region of salvinorin A binding—Tyr 7.35 and Tyr 7.36, which were experimentally proposed as essential for salvinorin binding<sup>49</sup>—are replaced by Trp and His, respectively. Also, some other residues in the closest neighborhood, particularly in VI and VII helices, are different. Other differences located in spatial proximity of the crucial residues are of minor importance.

The pose of salvinorin A alone derived from docking satisfies most contacts suggested by experiments and is characterized by spatial proximity of the ligand's acetyl moiety and Cys 7.38. This was assumed to be one of the key contacts, since hydrolysis of the ester group results in a derivative called salvinorin B, deprived of KOR agonist activity.<sup>52</sup> Moreover, its interaction with Cys 7.38 was experimentally suggested<sup>53</sup> (Figure 2). The chosen position is also compatible with the recent hypothesis describing a putative binding region of salvinorin and its derivatives.<sup>54</sup> It seems to be more accordant to recently published data than earlier models.<sup>55,56</sup> The importance of Tyr 7.43 for salvinorin A action suggests that the binding pocket of salvinorin A and herkinorin could partially overlap with the orthosteric binding site, which is reflected in the results of salvinorin docking to apo- and DAMGO-bound receptor. In the latter case the hypothetical salvinorin pocket is partially occupied by the Phe-Gly-ol part of DAMGO.

On the other hand herkinorin, a salvinorin-based compound acts as a selective MOR agonist with nanomolar efficacy.<sup>57</sup> Structure similarity of both receptors and their potent atypical ligands allows for the assumption that the interaction occurs in

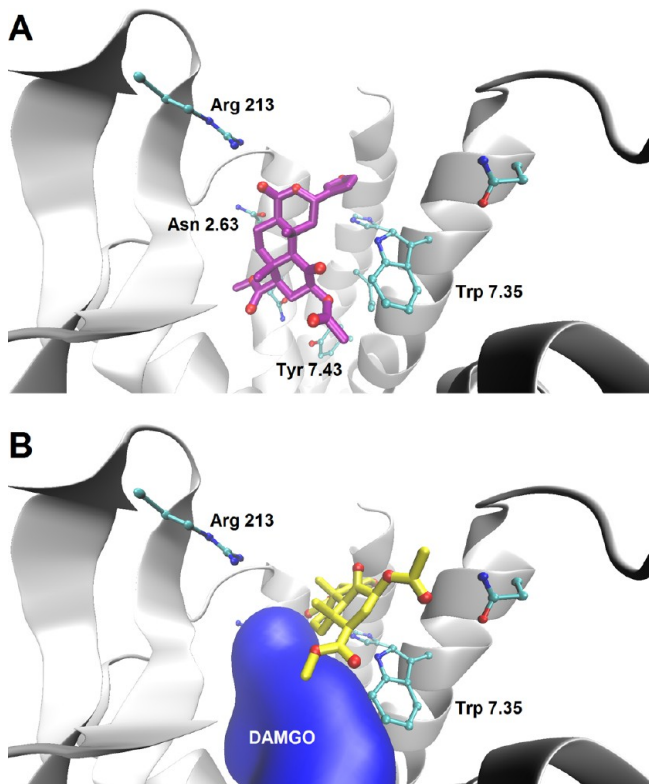


**Figure 2.** Docking poses of salvinorin A alone (A) and with DAMGO in orthosteric site (B). Hydrogen atoms omitted for clarity.

an analogous manner (Figure 3). It suggests a presence of a potent allosteric site at MOR that allows for its modulation and

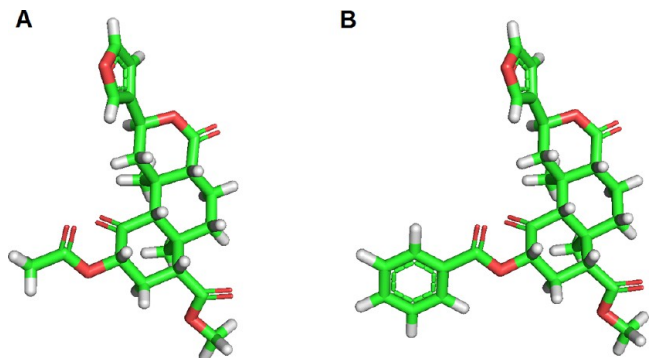


**Figure 3.** Comparison of salvinorin A (A) and herkinorin (B) structure.

activation. The site location would be analogous to salvinorin binding site in KOR. Docking results of herkinorin were to a considerable extent consistent with those of salvinorin. Poses satisfying criterion of proximity of 2-benzoyl moiety and Cys 7.38 residue were chosen and further assessed for similarity to salvinorin A contacts and regarding scoring function values (five scoring functions in the Sybyl software (D-Score, PMF-Score, G-Score, ChemScore, and F-Score) or the scoring function in the Glide program (GlideScore)).

To our knowledge, for THC and cannabidiol no experimental evidence for allosteric binding site location is available to date. Docking positions for these compounds were chosen on the basis of scoring functions and visual inspection. A large part of well-scored results shared the same space with

that of salvinorin A, which could suggest a common allosteric binding region for lipophilic terpene ligands. As the results of cannabinoids docking to both apo- and DAMGO-bound receptor were very similar, the latter poses were picked for further examination for clarity. The putative binding pocket consists of Trp (7.35), His (7.36), Thr (7.32), Tyr (2.64), Ile (1.35), Ala (1.32), Thr (1.31), Ser (1.28), and Lys (6.58).

All the allosteric modulators were docked to both unliganded and DAMGO-bound protein. The DAMGO was chosen as an orthosteric ligand according to original experimental data, where it was used as an agonist. It is important since allosteric effects are probe-specific.<sup>58</sup>

Docking poses of morphine and DAMGO were chosen on the basis of abundant experimental data and related work,<sup>59</sup> as well as on scoring functions values. In particular, the Asp 149 (3.32), which is conserved among aminergic GPCRs, was adopted as an anchor point for the protonated nitrogen of agonists, and the His 299 (6.52) was expected to interact with their phenolic groups. The main contacts are presented in Figure 4.

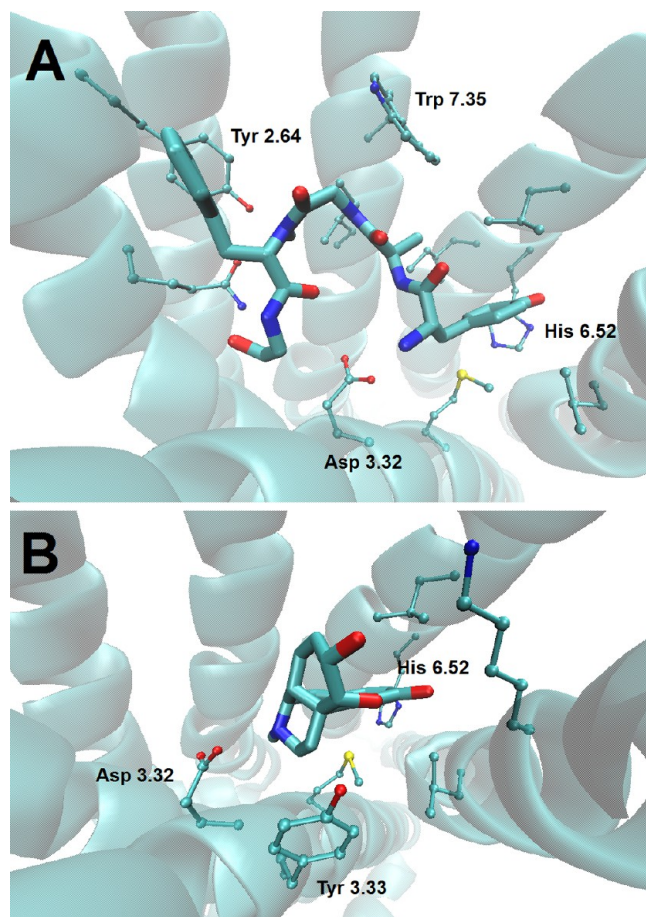


**Figure 4.** Docking positions of DAMGO (A) and morphine (B). Hydrogen atoms omitted for clarity.

## ■ MOLECULAR DYNAMICS

**Environment.** The function of a transmembrane receptor cannot be considered without the influence of the surrounding membrane, which was also proven for MOR.<sup>60</sup> There are reports on both importance of membrane lipid composition for receptor function and of its proper imitation in simulations.<sup>61,62</sup>

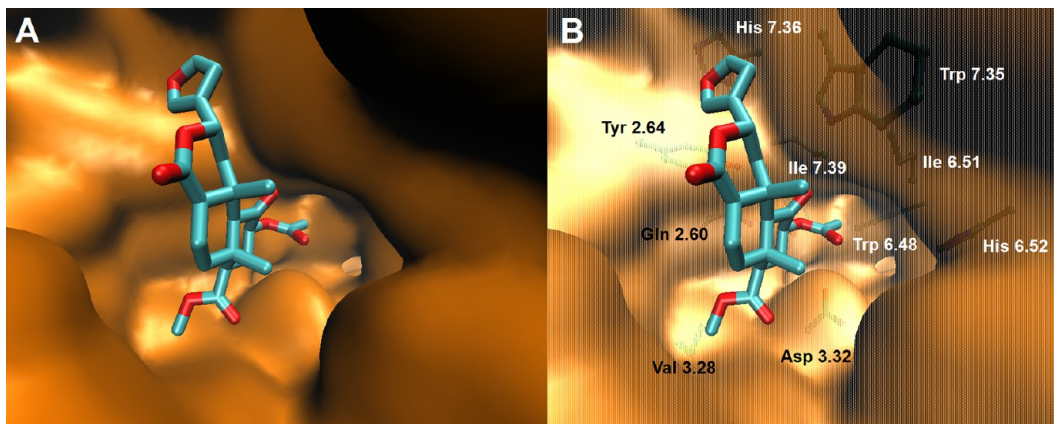
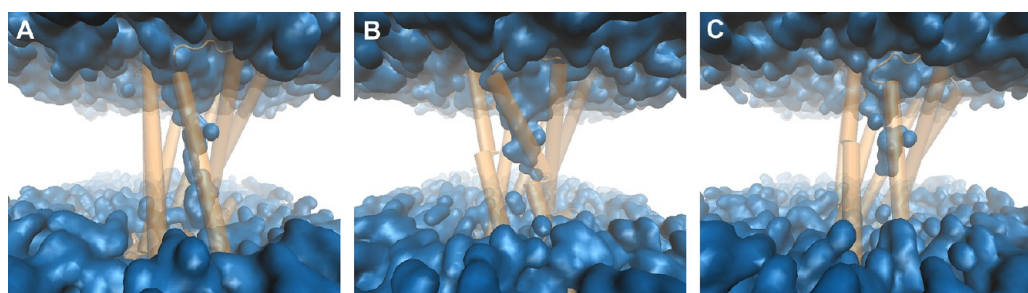


**Figure 5.** Shape of the salvinorin A binding pocket after simulation in the raftlike membrane (simulation 51): (A) Solid surface representation depicting cavity in the nearness of 2-acetyl moiety of salvinorin, (B) Transparent surface representation with side chain description.



basically less water molecules in the channel with DAMGO and cannabidiol bound.

**Figure 6.** Final snapshots of the receptor-spanning water chain formed after DAMGO binding in MOR (A), closed hydrophobic barrier in apo-MOR (B), and that in MOR with DAMGO and cannabidiol bound (C).

reason why  
different  
membrane  
compositions  
were explored.

Furthermore, as the allosteric effect of salvinorin A and cannabinoids on MOR is weak, their mechanisms of action were expected to be difficult to identify and likely to be blurred by simplifications usually applied in MD of GPCRs. Therefore, we decided to construct native-like systems. Membrane composition was based on results of experiments on neural cell rafts, where activated ORs tend to migrate,<sup>63</sup> whereas active-state MOR was modeled in a complex with G<sub>s</sub> protein.<sup>31</sup> Although all these conditions have been applied separately to GPCRs,<sup>64,65</sup> this is, to our knowledge, the first report on MD of active-state GPCR homology model in complex with G-protein immersed in a raftlike membrane, providing a high level of system complexity and native-likeness. For comparison, a series of MD simulations of ligand–receptor complexes immersed in simple membranes, i.e. pure POPC, POPC + 20% of cholesterol, and 40% of cholesterol were performed (Table 1) so that comparison of membrane influence was possible.

Since sodium ions are proven to affect GPCR activation, 0.15 M NaCl was used as an ionic component. In all simulations of the apo form of MOR sodium ion migration toward the Asp 2.50 was observed, as described earlier.<sup>8,9</sup>

**Model Selection.** First simulated sets contained unliganded protein, protein in complex with DAMGO or with morphine immersed in raftlike membrane. All simulations of unbound or morphine-bound receptor were similar. Therefore, DAMGO simulations became a decisive factor for the selection of models. In this configuration, representative of the population based on fully activated templates and mouse MOR structure (described as population E in the original modeling paper) have shown significantly better stability and compatibility with experimental results. Thus, it was selected for further computations, which

included the simulations of the receptor with a modulator alone or the modulator and DAMGO bound simultaneously and additional simulations of the receptor with herkinorin bound.

**Repetitions.** Instead of performing molecular dynamics as replicas of exactly the same systems with only different random seeds, the validation of simulations was carried out using several different, longer simulations by reasoning from similarities and differences between systems. In fact, the spectrum of performed simulations can be considered as a series of repetitions in two dimensions: (1) simulations of the same complexes (morphine, DAMGO, salvinorin A, DAMGO, and salvinorin A and the apo-form of the receptor) in different membrane environments and (2) the same membrane compositions tested with different protein–ligand complexes. As an example of the first approach, final coordinates of salvinorin A in DAMGO-bound receptor are similar despite various environments, with one outlying result in the most fluid, the least native-like membrane. Such convergence indicates that the salvinorin A probably exerts affinity to this place. Morphine, a partial MOR agonist, did not promote water chain formation in any environment, indicating that this effect of morphine on MOR is more universal and not restricted to particular conditions. The second dimension, on the other hand, provided insight in differences between dense and liquid membranes, e.g. as described for DAMGO behavior. In particular, similarities between raft-like and 20% cholesterol membranes were noticed.

This strategy made results analysis more difficult, yet allowed exploration of longer time scales and drawing of more general conclusions within the same computational budget.

**Ligand Interactions.** The orthosteric ligands were stable in their binding pocket. Morphine remained in its starting position

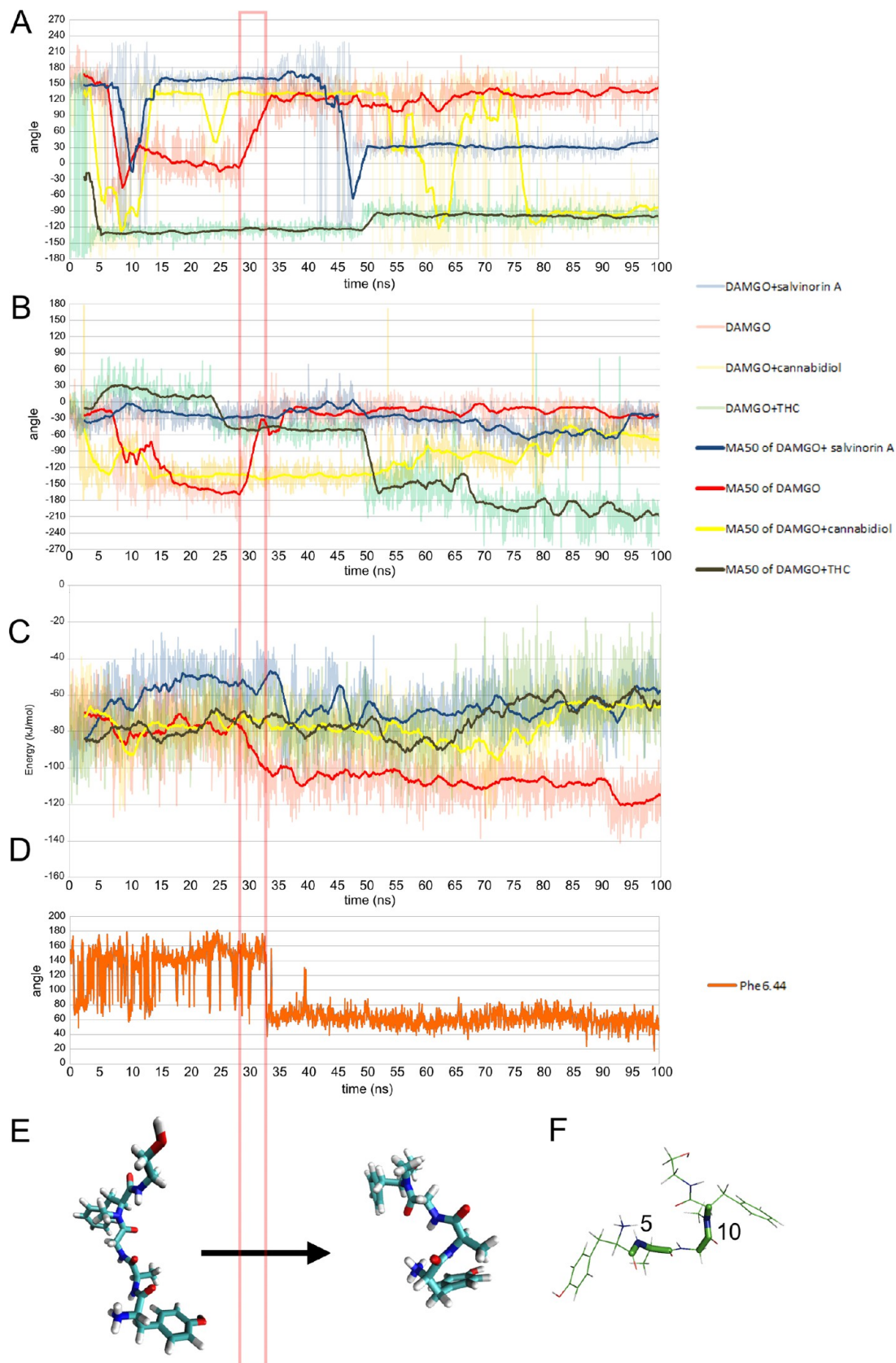


**Figure 7.** DAMGO reorganization in simulation of MOR-DAMGO complex in raft-like membrane: (A) change in the dihedral 5; (B) change in dihedral 10; (C) change in DAMGO internal interactions energy; (D) rotameric transition of Phe 6.44; (E) DAMGO conformational change; (F) reference numbers for dihedrals. MA50—moving average of 50 steps.

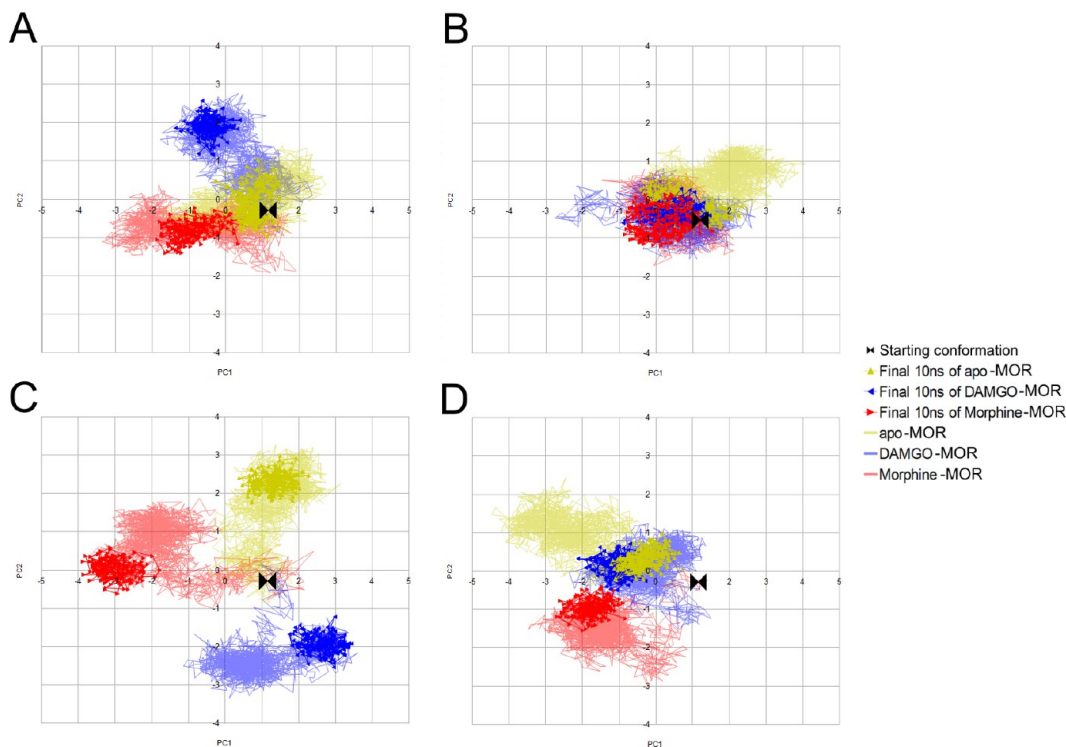


**Figure 8.** First two principal components of morphine-MOR, DAMGO-MOR, and the apo-MOR trajectories in four membranes in the common subspace. The plot is presented in four parts for clarity. (A) raftlike membrane, (B) POPC membrane, (C) 20% CHL membrane, (D) 40% CHL membrane.

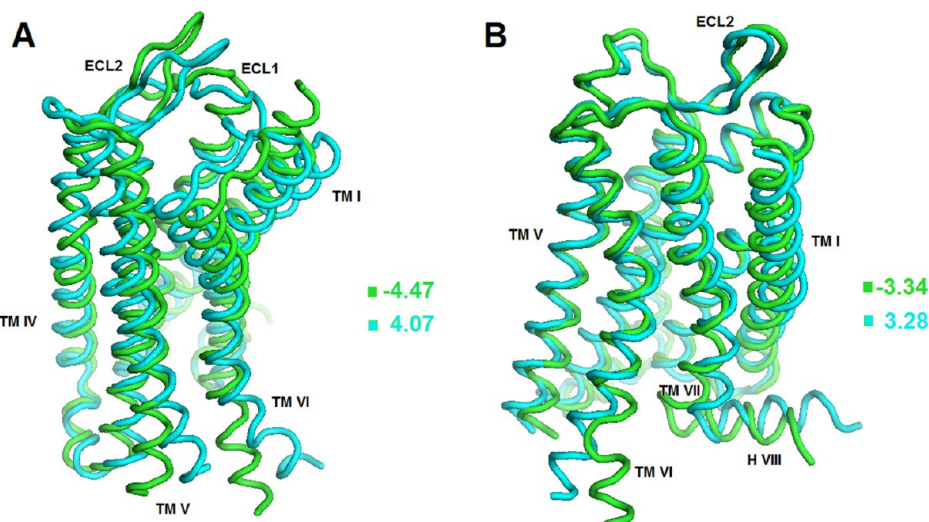


**Figure 9.** Trajectory projections on the average structure resulting from PCA of morphine-MOR, DAMGO-MOR, and the apo-MOR trajectories in four membranes. Projections correspond to extreme values along the first (A) and the second (B) PC. The frames exaggerate occurring changes and do not show exact simulation snapshots. The legend corresponds to PC values from the Figure 8.

Validation that docking is valid

in all membranes. DAMGO, as a flexible ligand, adopted a wider spectrum of possible conformations. Nevertheless, the salt bridge between its protonated nitrogen and Asp 149 (3.32), as well as interaction with His 299 (6.52) were stable in all simulations.

As salvinorin A starting positions were different in the apo- and DAMGO-bound protein due to altered steric conditions (Figure 2), different effects were observed. Salvinorin A bound to MOR immersed in raft membrane (reference number S1 in the Table 1) drifted slightly deeper into the receptor and remained there to the end of the simulation. The position

resembled other computational predictions<sup>54</sup> and involved aromatic stacking of the furanone ring mainly with His 7.36, Trp 7.35, and Tyr 2.64. The 2-acetyl moiety of salvinorin A is anchored at Ile 7.39. The bulky Trp 7.35 interrupts the development of better hydrophobic interaction with Ile 7.39 sterically. As mentioned, there is tyrosine at the 7.35 position in KOR, which has smaller and more flexible side chain. Comparison with  $\delta$  opioid receptor (DOR) structure (PDB ID: 4EJ4<sup>66</sup>) reveals that it lacks any aromatic side chain at the 7.35 position. Together, this indicates that residue 7.35 is

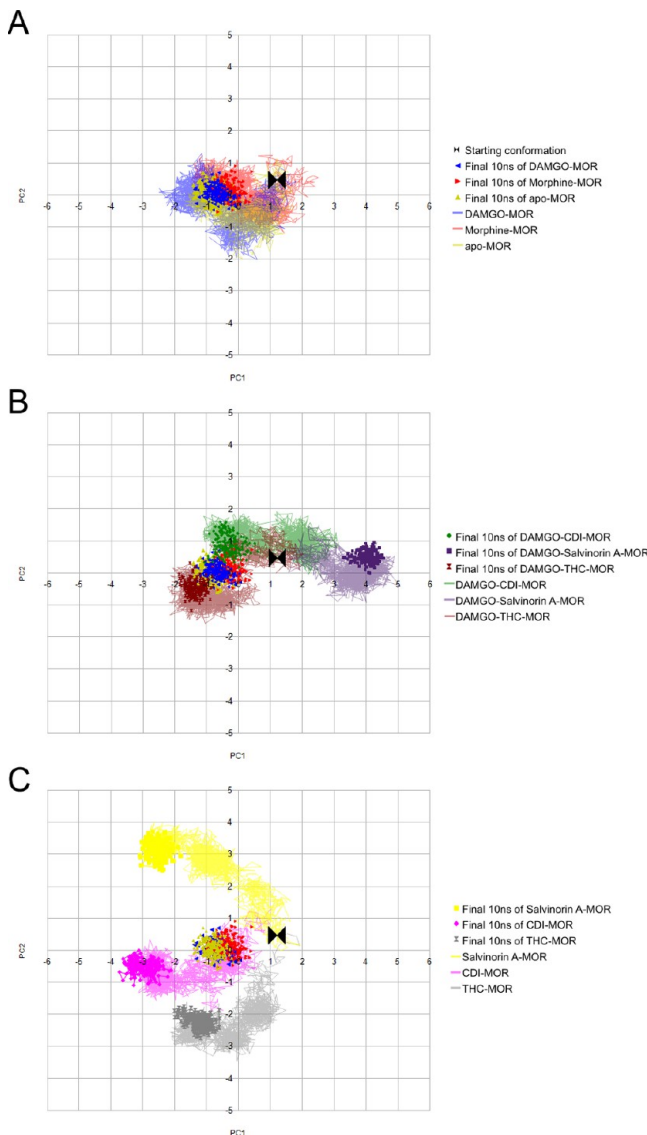


**Figure 10.** PCA of simulations performed in the raftlike membrane analyzed in the common subspace. The plot presenting the first two PCs is divided into three parts for clarity. (A) not modulated complexes, (B) simulations of the MOR with DAMGO and modulator bound simultaneously, (C) modulator–MOR systems.

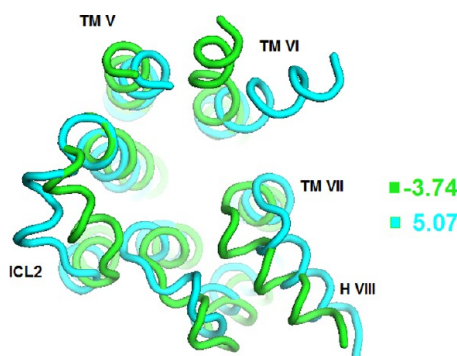


**Figure 11.** Trajectory projections on the average structure resulting from PCA of the complexes immersed in the raftlike membrane. Projections correspond to extreme values along the first PC. The legend corresponds to PC values from Figure 10.

these paragraphs are talking about the interactions that take place once the allosteric modulator are in place. Little value in reading this in depth since we are not working with allosteric modulators.

important for selective recognition of the OR subtype by neoclerodanes.

Interestingly, a cavity capable of accommodating a large planar substituent can be observed in the region of Trp 6.48, as shown in Figure 5. The cavity borders directly with 2-acetyl moiety of the ligand. This could be related to the activity of herkinorin and other 2-aryl-substituted derivatives of the salvinorin scaffold.<sup>67</sup>

The assumption of 2-benzoyl moiety fitting the mentioned cavity has interesting consequences regarding signaling bias at MOR. It was shown by Tidgewell et al. that in contrast to 2-benzoyl derivatives of salvinorin A, the 2-benzamide derivative promotes  $\beta$ -arrestin recruitment and internalization of MOR.<sup>68</sup> This means that change of noninternalizing ligand into internalizing one is caused by only changing ester into amide. The location of 2-substituent hypothesized above would mean that introduction of a hydrogen bond donor in the area, and consequently alteration of interactions with Tyr320 (7.43), Gln 115 (2.60), and Trp 6.48 would be essential for signaling bias. It was shown by Collu et al. that Trp 6.48 plays a role in differentiation of response to clozapine and desmethylclozapine at DOR.<sup>69</sup>

The position adopted by the furan ring is consistent with the structure–activity relationship of 15- and/or 16-substituted salvinorin analogues at KOR.<sup>70</sup> A vast majority of such modifications would violate steric restraints, protrude in the direction of the surrounding charged side chains or decrease stacking. In contrast, a 16-alkyne substituent would improve  $\pi$  interactions without introducing steric incompatibility, which is reflected in improved 16-alkyne-salvinorin A binding to KOR.

The described behavior of salvinorin, mostly pronounced in the raft membrane, was observed also in simulation 53. Furthermore, in these two systems emergence of a stable water chain spanning the 7TM bundle was observed, which is believed to be a hallmark of receptor activation.<sup>10</sup> This is in contrast to systems 52 or 54, where the water channel was disrupted.

Among simulated salvinorin A-DAMGO-MOR complexes, the most common phenomenon was the modulator migration toward the TM I-TMVII interface. Only in the complex in the POPC membrane (82) salvinorin A remained in the starting position. The final binding pocket generally consisted of Tyr 2.64, Gly 2.67, His 7.36, Thr 7.32, Gln 7.31, Glu 312 from ECL3, Ser 1.28, Met 1.29, Thr 1.31 and Ala 1.32.

Simulation of the herkinorin (41) was affected by its initial position. As positions of 2-substituents and furan rings were similar for herkinorin and salvinorin A, similar behavior was expected. Surprisingly the benzoyl moiety of herkinorin served as an anchor in the initial position, directly contacting Cys 7.38 and stacked between Trp 7.35 and Tyr 6.54. This may suggest that the benzoyl moiety plays an important role not only in recognition and shape complementarity but also in stabilizing intermediate binding states.

The investigated cannabinoids drifted toward the TM I-TM VII in simulations 61, 91, and 101 similarly to salvinorin A. The final binding pocket was identical as that of salvinorin A after migration when DAMGO was present. A greater difference can be observed in systems where DAMGO is absent, i.e. 61 and 71. THC in 61 drifted apart from TM VII and eventually located near the pocket described above. On the other hand, cannabidiol in 71 remained in its docking position for all the production run, establishing hydrogen bonds with Asn 2.63 and Trp 7.35 and aromatic stacking interactions with Tyr 2.64.

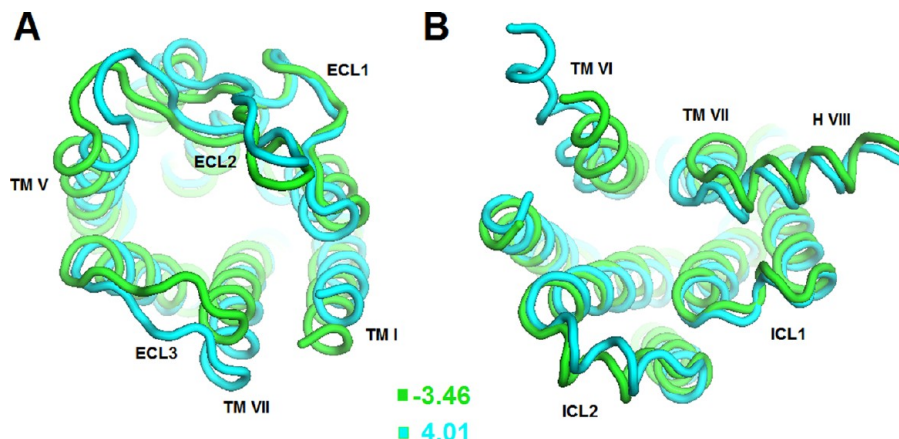


**Figure 12.** Trajectory projections on the average structure resulting from PCA of the complexes immersed in the raftlike membrane. Projections correspond to extreme values along the second PC. (A) motions of the extracellular part of the 7TM domain, (B) motions of the intracellular part of the receptor. The legend corresponds to PC values from Figure 10.

Interestingly, THC adopted a similar position after 9.09 ns of simulation and remained there for 23 ns before drifting farther. The observation can be connected with the more rigid structure of THC and may be related to cannabidiol negative allosteric modulation activity being 6-fold higher than that of THC.

**Intrapeptide Transmembrane Water Chain.** There is increasing evidence for a role of intrapeptide membrane-spanning water chain formation in protein activation.<sup>10</sup> It is assumed to emerge after breakdown of the “hydrophobic barrier” at the intracellular part of GPCRs.<sup>71,72</sup> Analysis of 7TM bundle interior in simulations revealed various responses to agonists, modulators and sodium ions. In the raftlike membrane, the presence of DAMGO in the orthosteric site in simulation 31 promoted breakdown of the hydrophobic barrier and water chain creation, while it was not observed in simulation of apo-MOR (11) or when a cannabinoid modulator was bound (61, 71, 91, 101) (Figure 6). Interestingly, modulators decreased also overall exchange of water in the orthosteric binding pocket and increased the fraction of very long-resident water molecules (Table S3), which is in accordance with data obtained by Yuan et al.<sup>8</sup> Salvinorin A exerted similar effect also in simplified membranes (Table S4). In simulations with DAMGO and MOR immersed in simplified membranes, simulation 33 result resembles that of 31, while in 32 and 34 the chain was formed only temporarily and easily disrupted.

Salvinorin A action was exceptional among modulators, since it enforced the chain formation (81), and moreover it promoted the phenomenon on its own (51). A similar effect was also observed in simplified membranes. Interestingly, the chain appeared in apo-MOR in complexes 12 and 13, but not in 11 and 14. This discrepancy points that probably water chain was easier to form in more fluid membranes. Morphine did not induce water chain formation in any system, while herkinorin promoted establishment of water chain bypassing the hydrophobic barrier. In general, number of similarities between systems in membranes of moderate rigidity (raft-like and 20% cholesterol) was observed, as described above and in the PCA section. The most fluid and the most rigid membrane-immersed systems (pure POPC and 40% cholesterol, respectively) presented mostly outlying properties.

Various effects of agonists can result from different mechanisms of activation employed. DAMGO is an internalizing agonist, which is in opposition to morphine<sup>73</sup> and

different MOR behavior in membrane upon activation by these two agonists was described.<sup>74</sup> In turn, herkinorin is a noninternalizing agonist<sup>75</sup> and is assumed to bind in a pocket different than that of morphine or DAMGO. The lack of the effect in the case of morphine suggests that it employs different activation mechanism or that allosteric effect of  $G_s$  protein interferes with morphine action.

The result of salvinorin simulations suggests the negative modulation mechanism different from that of cannabinoids. Decrease in DAMGO binding can be explained partially by modulation via common allosteric pocket for lipophilic modulators at the top of TM I–II–VII. However, it can also result from the spatial overlap of DAMGO and salvinorin A binding pockets. The simulation 51 shows that despite the lack of agonist activity, salvinorin A can stably interact with neoclerodane binding pocket and, in favorable conditions, exert some effects. In this particular case, allosteric effect of coupled  $G$  protein as well as membrane environment can be accounted for such conditions. Interestingly, small-particle opiates possibly would not interfere sterically with salvinorin A, and hypothetically, the effect of modulator cobinding could be different.

**DAMGO Relaxation.** Analysis of intramolecular interactions within the DAMGO molecule revealed its different behavior in negatively modulated and modulator-free complexes. The presence of any modulator prevented DAMGO from adopting the lowest energy conformation (Figure 7C). Modulators restrict DAMGO movements, inhibiting some conformer transitions. In particular, two dihedrals (Figure 7A—dihedral 5—and B—dihedral 10) change simultaneously in a single event in the nonmodulated complex 31 at the moment of energy change, which is not observed in the modulated systems. Interestingly, the observed phenomenon directly preceded rotameric transition of Phe 291 (6.44) as shown in Figure 7D. The residue subsequently lost contact with hydrophobic lock residues and allowed water particles to penetrate the receptor interior deeper. A similar mechanism was observed in simulation 81, where the Phe 6.44 rotameric transition was immediately followed by receptor-spanning water chain formation. It would suggest the relationship between the transmission switch and hydrophobic lock, constituting together a larger switch.

**Covariance and Principal Component Analysis.** In order to assess the correlations of movements of particular

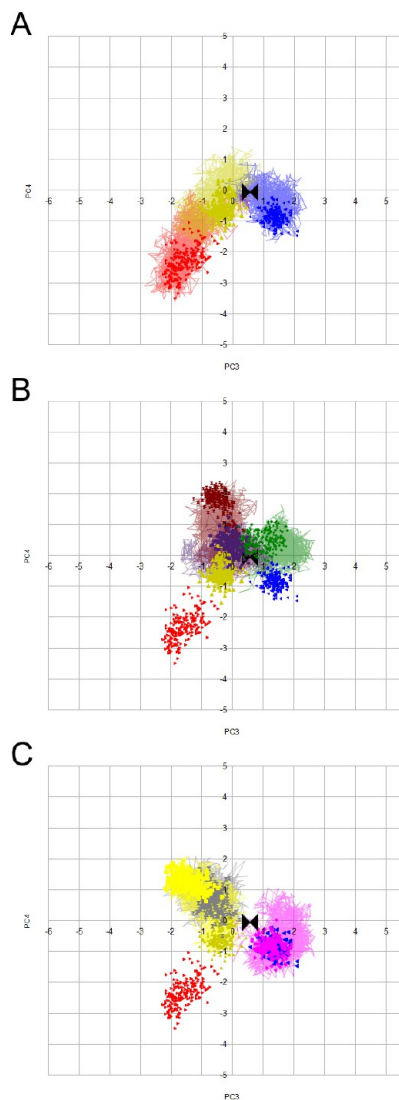


**Figure 13.** PCA of simulations performed in the raft-like membrane analyzed in the common subspace. The plot presenting the PC3 and PC4 is divided into three parts for clarity. (A) not modulated complexes, (B) simulations of the MOR with DAMGO and modulator bound simultaneously, (C) modulator-MOR systems.

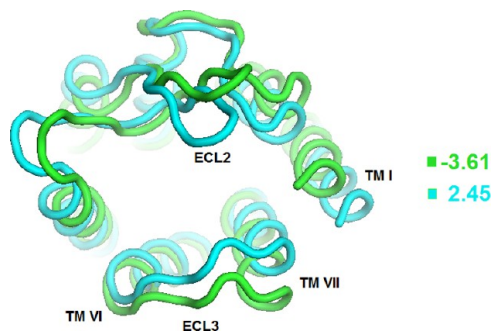


**Figure 14.** Trajectory projections on the average structure resulting from PCA of the complexes immersed in the raftlike membrane. Projections correspond to extreme values along the PC4. The legend corresponds to PC values from Figure 13.

protein domains, a covariance matrix can be constructed. Such matrices were created for simulations of receptor in raftlike membrane to investigate influence of modulators on correlated motions (Table S1). The procedure revealed some patterns that are compliant with the other analyses. In general, modulator binding un harnesses linear correlations observed in agonist-bound receptor simulations. The differences mostly concern silenced covariance of TM I-II and an agonist with ICL3 and intracellular part of TM VI in modulator-containing systems.

In order to verify the generality of observed phenomena and to get deeper insight into their nature, a PCA was performed. Simulations were analyzed in groups. This allowed for comparison of trajectories in common subspaces. 7TM backbone without N terminus and ICL3 was analyzed. The first analysis concerned complexes of the orthosteric agonists and the apo-MOR in four membranes. The analysis reveals some general patterns (Figure 8). First two PCs contain several motions, presented in Figure 9 as the two extreme projections along a trajectory on the average structure (It should be noted that the projections present artificial structures from PCA. They exaggerate occurring changes and do not show exact simulation snapshots). A plot of these PCs shows that simulations in the most fluid and the most rigid membrane do not differentiate well between different ligands and the unliganded protein. In both the POPC and 40% CHL membranes all complexes explore similar conformational space, particularly in the last 10 ns of simulations. In turn, complexes in membranes with intermediate rheological properties are reasonably separated. In general, in these two membranes agonists mostly promote conformational change described by decrease in PC1 value, which includes outward movement of ECLs and move of intracellular part of TM V and TM VI toward TM IV. It is worth emphasizing that in terms of the first two PCs, morphine demonstrates similar PC1 drift in almost all systems (except of that in the pure POPC membrane). It is reasonable that interactions of morphine, which is a small, rigid agonist are less affected by environment than a flexible agonist or a modulator. Therefore, the motions described by the decrease in PC1 value can be considered as a relevant effect of agonist interaction. In the light of this observation, simulation in the raftlike membrane (Figure 8A) describes the DAMGO behavior more appropriately than that in 20% CHL membrane (Figure 8C). Another interesting remark is that in this PCA all the complexes in the most rigid, 40% CHL membrane exhibit decrease in PC1 to some extent (Figure 8D). It corresponds to reports describing MOR propensity to stay in rigid lipid raft environment when activated.<sup>63</sup>

All systems in the raftlike and 20% CHL membranes behave similarly in terms of PC3/PC4 (Figure S1). The explanation of the corresponding motions is presented in Figure S2.

The second group analysis concerned complexes in the raftlike membrane. The analysis revealed that the first PC was very strongly affected by motions induced by herkinorin. Therefore, we decided to exclude herkinorin from the set and perform another PCA. The second approach has shown that the first and the second PCs are dominated by modulator-induced effects (Figure 10). All nonmodulated systems explore the same conformational space in terms of PC1/PC2, especially during the last 10 ns of simulations. Also the complexes modulated by cannabinoids present only slight differences from not modulated systems. The most pronounced effect is visible in all the modulator-MOR as well as salvinorin A-DAMGO-

what phenomena?

This is the argument & validation that the different membrane composition does NOT matter.

MOR complexes. It is clearly visible that the effects of both cannabinoids are similar and partially different from that of salvinorin A. All modulator-MOR complexes show decrease in the first PC, which corresponds mostly to the closing of 7TM intracellular interface (Figure 11). It is in opposition to salvinorin A-DAMGO-MOR, which shows increased value of the PC1. The second PC describes differences between cannabinoid-MOR and salvinorin A-MOR. THC and cannabidiol promote the decrease in distances between extracellular loops (Figure 12A) and an inward movement of TM VI (Figure 12B), while salvinorin A exerts the opposite effect. Also PC4 show apparent division on modulated and not modulated systems (Figure 13). Changes in distances between ECLs are shown in Figure 14.

## CONCLUSIONS

The obtained results suggest a shared binding region for lipophilic allosteric ligands, reveal possible differences in modulation mechanism between cannabinoids and salvinorin A, and show ambiguous properties of the latter. A possible common binding site for lipophilic terpene MOR allosteric modulators is identified in the top of the TM I-TM II-TM VI interface. Another possible pocket specific for neoclerodanes, their putative binding mode, and bases for their pathway selectivity are suggested. These data provide a relevant reference for structure-based drug design methods, facilitating elaboration of novel modulators and biased ligands.

The cannabinoid binding restrain DAMGO flexibility in the orthosteric binding pocket, decreasing its ability to induce intrareceptor transmembrane water chain formation. PCA indicates that cannabinoids induce closing of intra- and extracellular receptor interfaces by inward motions of TM VI, TM VII, and H VIII as well as intra-and extracellular loops. This is in opposition to action of agonists, which promote the receptor opening. Salvinorin A action is equivocal. Its binding space overlaps with the orthosteric binding pocket and interferes with DAMGO. This could be one of the probable mechanisms of decrease in DAMGO binding. Another is that salvinorin A can be displaced upon agonist binding to a common terpenoid pocket where it exerts further negative modulation. Yet, molecular dynamics suggest the possibility of salvinorin A negatively modulating DAMGO binding and positively modulating DAMGO-induced activation, which is implied by water chain formation, PCA, and covariance analysis. Moreover, salvinorin A induce some vistas of activation in favorable environment.

A single event of DAMGO conformational transition was caught in simulation performed in raftlike membrane. The observed sequence of related events provides possible explanation of DAMGO action in the binding pocket and joins transmission switch, hydrophobic barrier breakdown, and intraprotein continuous water chain formation into one large mechanism.

The results emphasize the importance of the native-like environment in molecular dynamics simulations and uncover relationships between modulator and orthosteric ligand binding and receptor behavior.

## ASSOCIATED CONTENT

### Supporting Information

The Supporting Information is available free of charge on the ACS Publications website at DOI: [10.1021/acs.jcim.Sb00280](https://doi.org/10.1021/acs.jcim.Sb00280).

Covariance matrices for simulations performed in raftlike membrane. Plots of PC3 and PC4 from PCA of morphine-MOR, DAMGO-MOR, and the apo-MOR complexes in four membranes. Trajectory projections on the average structure resulting from PCA of the morphine-MOR, DAMGO-MOR, and the apo-MOR complexes immersed in the raftlike membrane, corresponding to extreme values along the PC3 and PC4. (PDF)

## AUTHOR INFORMATION

### Corresponding Author

\*Tel.: +48815357365. Fax: +48815357366. E-mail: [damian.bartuzi@gmail.com](mailto:damian.bartuzi@gmail.com), [damian.bartuzi@umlub.pl](mailto:damian.bartuzi@umlub.pl).

### Notes

The authors declare no competing financial interest.

## ACKNOWLEDGMENTS

The paper was developed using the equipment purchased within the project “The equipment of innovative laboratories doing research on new medicines used in the therapy of civilization and neoplastic diseases” within the Operational Program Development of Eastern Poland 2007–2013, Priority Axis I modern Economy, operations I.3 Innovation promotion. The research was partially performed during the postdoctoral fellowship of A.A.K. at University of Eastern Finland, Kuopio, Finland, under a Marie Curie fellowship. The work was supported by the Foundation for Polish Science (TEAM 2009-4/5 Program). Calculations were partially performed under a computational grant by Interdisciplinary Center for Mathematical and Computational Modeling (ICM), Warsaw, Poland, grant number G30-18, and under resources and licences from CSC, Finland. We acknowledge that the results of this research have been achieved using the PRACE-3IP project ALLOTRANS (FP7 RI-312763) resource Archer, based in the UK at the University of Edinburgh. Special thanks to Karol Sowiński for remarks and help in text redaction. Special thanks to Dr. Ewelina Bartuzi for suggestions regarding PCA analysis.

## ABBREVIATIONS

GPCRs, G-Protein Coupled Receptors; TM, transmembrane domain; 7TM, seven transmembrane domain; ICL, intracellular loop; ECL, extracellular loop; OR, opioid receptor; MOR,  $\mu$  opioid receptor; CADD, computer aided drug design; MD, molecular dynamics; THC, tetrahydrocannabinol; CDI, cannabidiol; POPC, 1-palmitoyl-2-oleyl-sn-glycero-3-phosphocholine; CHL, cholesterol; SM, sphingomyelin; POPE, 1-palmitoyl-2-oleyl-sn-glycero-3-phosphoethanolamine; GAFF, general amber force field; KOR,  $\kappa$  opioid receptor; DOR,  $\delta$  opioid receptor; H VIII, intracellular helix VIII; PCA, principal component analysis; PC, principal component

## REFERENCES

- (1) Luttrell, L. M. Minireview: More Than Just a Hammer: Ligand “Bias” and Pharmaceutical Discovery. *Mol. Endocrinol.* **2014**, *28*, 281–294.
- (2) Lane, J. R.; Donthamsetti, P.; Shonberg, J.; Draper-Joyce, C. J.; Dentry, S.; Michino, M.; Shi, L.; López, L.; Scammells, P. J.; Capuano, B.; Sexton, P. M.; Javitch, J. A.; Christopoulos, A. A New Mechanism of Allostery in a G protein-coupled Receptor Dimer. *Nat. Chem. Biol.* **2014**, *10*, 745–752.

- (3) Ghanemi, A. Targeting G protein coupled receptor-related pathways as emerging molecular therapies. *Saudi Pharm. J.* **2015**, *23*, 115–129.
- (4) Drews, J. Drug Discovery: a Historical Perspective. *Science* **2000**, *287*, 1960–1964.
- (5) Fredriksson, R.; Lagerström, M. C.; Lundin, L. G.; Schiöth, H. B. The G-protein-coupled Receptors in the Human Genome Form Five Main Families. Phylogenetic Analysis, Paralogon Groups, and Fingerprints. *Mol. Pharmacol.* **2003**, *63*, 1256–72.
- (6) Kolakowski, L. F., Jr. GCRDb: a G-protein-coupled Receptor Database. *Recept. Channels* **1994**, *2*, 1–7.
- (7) Pelé, J.; Abdi, H.; Moreau, M.; Thybert, D.; Chabbert, M. Multidimensional Scaling Reveals the Main Evolutionary Pathways of Class A G-protein-coupled Receptors. *PLoS One* **2011**, *6*, e19094.
- (8) Yuan, S.; Vogel, H.; Filipek, S. The Role of Water and Sodium Ions in the Activation of the m-Opioid Receptor. *Angew. Chem., Int. Ed.* **2013**, *52*, 10112–10115.
- (9) Shang, Y.; LeRouzic, V.; Schneider, S.; Bisignano, P.; Pasternak, G. W.; Filizola, M. Mechanistic Insights into the Allosteric Modulation of Opioid Receptors by Sodium Ions. *Biochemistry* **2014**, *53*, 5140–5149.
- (10) Yuan, S.; Filipek, S.; Palczewski, K.; Vogel, H. Activation of G-protein-coupled Receptors Correlates with the Formation of a Continuous Internal Water Pathway. *Nat. Commun.* **2014**, *5*, 4733.
- (11) Dror, R. O.; Green, H. F.; Valant, C.; Borhani, D. W.; Valcourt, J. R.; Pan, A. C.; Arlow, D. H.; Canals, M.; Lane, J. R.; Rahmani, R.; Baell, J. B.; Sexton, P. M.; Christopoulos, A.; Shaw, D. E. Structural Basis for Modulation of a G-protein-coupled Receptor by Allosteric Drugs. *Nature* **2013**, *503*, 295–299.
- (12) Abdul-Ridha, A.; López, L.; Keov, P.; Thal, D. M.; Mistry, S. N.; Sexton, P. M.; Lane, J. R.; Canals, M.; Christopoulos, A. Molecular Determinants of Allosteric Modulation at the M1 Muscarinic Acetylcholine Receptor. *J. Biol. Chem.* **2014**, *289*, 6067–6079.
- (13) Manglik, A.; Kruse, A. C.; Kobilka, T. S.; Thian, F. S.; Mathiesen, J. M.; Sunahara, R. K.; Pardo, L.; Weis, W. I.; Kobilka, B. K.; Granier, S. Crystal Structure of the M-opioid Receptor Bound to a Morphinan Antagonist. *Nature* **2012**, *485*, 321–326.
- (14) Shim, J.; Coop, A.; MacKerell, A. D., Jr. Molecular Details of the Activation of the  $\mu$  Opioid Receptor. *J. Phys. Chem. B* **2013**, *117*, 7907–7917.
- (15) Provasi, D.; Artacho, M. C.; Negri, A.; Mobarec, J. C.; Filizola, M. Ligand-Induced Modulation of the Free-Energy Landscape of G Protein-Coupled Receptors Explored by Adaptive Biasing Techniques. *PLoS Comput. Biol.* **2011**, *7*, e1002193.
- (16) Kathmann, M.; Flau, K.; Redmer, A.; Tränkle, C.; Schlicker, E. Cannabidiol is an Allosteric Modulator at Mu- and Delta-opioid Receptors. *Naunyn-Schmiedeberg's Arch. Pharmacol.* **2006**, *372*, 354–361.
- (17) Rothman, R. B.; Murphy, D. L.; Xu, H.; Godin, J. A.; Dersch, C. M.; Partilla, J. S.; Tidgewell, K.; Schmidt, M.; Prisinzano, T. E. Salvinorin A: Allosteric Interactions at the m-Opioid Receptor. *J. Pharmacol. Exp. Ther.* **2007**, *320*, 801–810.
- (18) Burford, N. T.; Clark, M. J.; Wehrman, T. S.; Gerritz, S. W.; Banks, M.; O'Connell, J.; Traynor, J. R.; Alt, A. Discovery of Positive Allosteric Modulators and Silent Allosteric Modulators of the  $\mu$ -opioid Receptor. *Proc. Natl. Acad. Sci. U. S. A.* **2013**, *110*, 10830–10835.
- (19) Balsera, M. A.; Wriggers, W.; Oono, Y.; Schulten, K. Principal Component Analysis and Long Time Protein Dynamics. *J. Phys. Chem.* **1996**, *100*, 2567–2572.
- (20) Ng, H. W.; Laughton, C. A.; Doughty, S. W. Molecular Dynamics Simulations of the Adenosine A2a Receptor in POPC and POPE Lipid Bilayers: Effects of Membrane on Protein Behavior. *J. Chem. Inf. Model.* **2014**, *54*, 573–81.
- (21) Ng, H. W.; Laughton, C. A.; Doughty, S. W. Molecular Dynamics Simulations of the Adenosine A2a Receptor: Structural Stability, Sampling, and Convergence. *J. Chem. Inf. Model.* **2013**, *53*, 1168–78.
- (22) Kaczor, A. A.; Bartuzi, D.; Matosiuk, D. Modeling the Active Conformation of Human  $\mu$  Opioid Receptor. *Lett. Drug Des. Discovery* **2014**, *11*, 1053–1061.
- (23) Katoh, K.; Standley, D. M. MAFFT Multiple Sequence Alignment Software Version 7: Improvements in Performance and Usability. *Mol. Biol. Evol.* **2013**, *30*, 772–780.
- (24) Warne, A.; Moukhambetianov, R.; Baker, J. G.; Nehme, R.; Edwards, P. C.; Leslie, A. G. W.; Schertler, G. F. X.; Tate, C. G. The Structural Basis for Agonist and Partial Agonist Action on a  $\beta$ 1-adrenergic Receptor. *Nature* **2011**, *469*, 241–244.
- (25) Rasmussen, S. G.; Choi, H. J.; Fung, J. J.; Pardon, E.; Casarosa, P.; Chae, P. S.; Devree, B. T.; Rosenbaum, D. M.; Thian, F. S.; Kobilka, T. S.; Schnapp, A.; Konetzki, I.; Sunahara, R. K.; Gellman, S. H.; Pautsch, A.; Steyaert, J.; Weis, W. I.; Kobilka, B. K. Structure of a Nanobody-stabilized Active State of the b(2) Adrenoceptor. *Nature* **2011**, *469*, 175–180.
- (26) Rosenbaum, D. M.; Zhang, C.; Lyons, J. A.; Holl, R.; Aragao, D.; Arlow, D. H.; Rasmussen, S. G. F.; Choi, H. J.; Devree, B. T.; Sunahara, R. K.; Chae, P. S.; Gellman, S. H.; Dror, R. O.; Shaw, D. E.; Weis, W. I.; Caffrey, M.; Gmeiner, P.; Kobilka, B. K. Structure and Function of an Irreversible Agonist-b2 Adrenoceptor complex. *Nature* **2011**, *469*, 236–240.
- (27) Rasmussen, S. G.; DeVree, B. T.; Zou, Y.; Kruse, A. C.; Chung, K. Y.; Kobilka, T. S.; Thian, F. S.; Chae, P. S.; Pardon, E.; Calinski, D.; Mathiesen, J. M.; Shah, S. T.; Lyons, J. A.; Caffrey, M.; Gellman, S. H.; Steyaert, J.; Skiniotis, G.; Weis, W. I.; Sunahara, R. K.; Kobilka, B. K. Crystal Structure of the b2 Adrenergic Receptor-Gs protein Complex. *Nature* **2011**, *477*, 549–555.
- (28) Lebon, G.; Warne, T.; Edwards, P. C.; Bennett, K.; Langmead, C. J.; Leslie, A. G. W.; Tate, C. G. Agonist-bound Adenosine A2A Receptor Structures Reveal Common Features of GPCR Activation. *Nature* **2011**, *474*, 521–525.
- (29) Xu, F.; Wu, H.; Katritch, V.; Han, G. W.; Jacobson, K. A.; Gao, Z. G.; Cherezov, V.; Stevens, R. C. Structure of an Agonist-bound Human A2A Adenosine Receptor. *Science* **2011**, *332*, 322–327.
- (30) Eswar, N.; Marti-Renom, M. A.; Webb, B.; Madhusudhan, M. S.; Eramian, D.; Shen, M.; Pieper, U.; Sali, A. Comparative Protein Structure Modeling With MODELLER. In *Current Protocols in Bioinformatics*; John Wiley & Sons, Inc., 2006; Supplement 15, pp 5.6.1–5.6.30.
- (31) Chakrabarti, S.; Chang, A.; Gintzler, A. R. Subcellular Localization of Mu-opioid Receptor G(s) Signaling. *J. Pharmacol. Exp. Ther.* **2010**, *333*, 193–200.
- (32) Allen, F. H. The Cambridge Structural Database: a Quarter of a Million Crystal Structures and Rising. *Acta Crystallogr., Sect. B: Struct. Sci.* **2002**, *B58*, 380–388.
- (33) Spartan'10; Wavefunction, Inc.: Irvine, CA, 2010; [https://www.wavefun.com/products/windows/Spartan10/win\\_spartan.html](https://www.wavefun.com/products/windows/Spartan10/win_spartan.html).
- (34) SYBYL-X 1.3; Tripos International: St. Louis, MO, 2009.
- (35) Pike, L. J.; Han, X.; Chung, K.-N.; Gross, R. W. Lipid Rafts Are Enriched in Arachidonic Acid and Plasmenylethanolamine and Their Composition Is Independent of Caveolin-1 Expression: A Quantitative Electrospray Ionization/Mass Spectro metric Analysis. *Biochemistry* **2002**, *41*, 2075–2088.
- (36) Case, D. A.; Babin, V.; Berryman, J. T.; Betz, R. M.; Cai, Q.; Cerutti, D. S.; Cheatham, T. E.; Darden, T. A.; Duke, R. E.; Gohlke, H.; Goetz, A. W.; Gusarov, S.; Homeyer, N.; Janowski, P.; Kaus, J.; Kolossváry, I.; Kovalenko, A.; Lee, T. S.; LeGrand, S.; Luchko, T.; Luo, R.; Madej, B.; Merz, K. M.; Paesani, F.; Roe, D. R.; Roitberg, A.; Sagui, C.; Salomon-Ferrer, R.; Seabra, G.; Simmerling, C. L.; Smith, W.; Swails, J.; Walker, R. C.; Wang, J.; Wolf, R. M.; Wu, X.; Kollman, P. A. AMBER 14; University of California: San Francisco, 2014.
- (37) Wang, J.; Wang, W.; Kollman, P. A.; Case, D. A. Automatic Atom Type and Bond Type Perception in Molecular Mechanical Calculations. *J. Mol. Graphics Modell.* **2006**, *25*, 247–260.
- (38) Wang, J.; Wolf, R. M.; Caldwell, J. W.; Kollman, P. A.; Case, D. A. Development and Testing of a General AMBER Force Field. *J. Comput. Chem.* **2004**, *25*, 1157–1174.

- (39) Jämbeck, J. P. M.; Lyubartsev, A. P. Derivation and Systematic Validation of a Refined All-Atom Force Field for Phosphatidylcholine Lipids. *J. Phys. Chem. B* **2012**, *116*, 3164–3179.
- (40) Jämbeck, J. P. M.; Lyubartsev, A. P. An Extension and Further Validation of an All-Atomistic Force Field for Biological Membranes. *J. Chem. Theory Comput.* **2012**, *8*, 2938–2948.
- (41) Jämbeck, J. P. M.; Lyubartsev, A. P. Another Piece of the Membrane Puzzle: Extending Slipids Further. *J. Chem. Theory Comput.* **2013**, *9*, 774–784.
- (42) Vanquelef, E.; Simon, S.; Marquant, G.; Garcia, E.; Klimerak, G.; Delepine, J. C.; Cieplak, P.; Dupradeau, F.Y. R.E.D. Server: a Web Service for Deriving RESP and ESP Charges and Building Force Field Libraries for New Molecules and Molecular Fragments. *Nucleic Acids Res.* **2011**, *39*, W511–W517.
- (43) Sousa da Silva, A. W.; Vranken, W. F. ACPYPE - AnteChamber PYthon Parser interfacE. *BMC Res. Notes* **2012**, *5*, 367.
- (44) Wu, E. L.; Cheng, X.; Jo, S.; Rui, H.; Song, K. C.; Dávila-Contreras, E. M.; Qi, Y.; Lee, J.; Monje-Galvan, V.; Venable, R. M.; Klauda, J. B.; Im, W. CHARMM-GUI Membrane Builder Toward Realistic Biological Membrane Simulations. *J. Comput. Chem.* **2014**, *35*, 1997–2004.
- (45) Hess, B.; Kutzner, C.; van der Spoel, D.; Lindahl, E. GROMACS 4: Algorithms for Highly Efficient, Load-Balanced, and Scalable Molecular Simulation. *J. Chem. Theory Comput.* **2008**, *4*, 435–447.
- (46) R: A Language and Environment for Statistical Computing; R Foundation for Statistical Computing: Vienna, Austria, 2014; <http://www.R-project.org>.
- (47) Humphrey, W.; Dalke, A.; Schulten, K. VMD - Visual Molecular Dynamics. *J. Mol. Graphics* **1996**, *14.1*, 33–38, <http://www.ks.uiuc.edu/Research/vmd/>.
- (48) The PyMOL Molecular Graphics System, Version 1.5.0.4; Schrödinger, LLC, 2012.
- (49) Kane, B. E.; McCurdy, C. R.; Ferguson, D. M. Toward a Structure-based Model of Salvinorin A Recognition of the Kappa-opioid Receptor. *J. Med. Chem.* **2008**, *51*, 1824–30.
- (50) Ballesteros, J. A.; Weinstein, H. Integrated Methods for the Construction of Three Dimensional Models and Computational Probing of Structure-Function Relations in G-protein Coupled Receptors. *Methods Neurosci.* **1995**, *25*, 366–428.
- (51) Wu, H.; Wacker, D.; Mileni, M.; Katritch, V.; Han, G. W.; Vardy, E.; Liu, W.; Thompson, A. A.; Huang, X. P.; Carroll, F. I.; Mascarella, S. W.; Westkaemper, R. B.; Mosier, P. D.; Roth, B. L.; Cherezov, V.; Stevens, R. C. Structure of the Human  $\kappa$ -opioid Receptor in Complex with JDTic. *Nature* **2012**, *485*, 327–332.
- (52) Chavkin, C.; Sud, S.; Jin, W.; Stewart, J.; Zjawiony, J. K.; Siebert, D. J.; Toth, B. A.; Hufeisen, S. J.; Roth, B. L. Salvinorin A, an Active Component of the Hallucinogenic Sage *Salvia Divinorum* is a Highly Efficacious Kappa-opioid Receptor Agonist: Structural and Functional Considerations. *J. Pharmacol. Exp. Ther.* **2004**, *308*, 1197–1203.
- (53) Yan, F.; Bikbulatov, R. V.; Mocanu, V.; Dicheva, N.; Parker, C. E.; Wetsel, W. C.; Mosier, P. D.; Westkaemper, R. B.; Allen, J. A.; Zjawiony, J. K.; Roth, B. L. Structure-based Design, Synthesis, Biochemical and Pharmacological Characterization of Novel Salvinorin A Analogues as Active State Probes of the  $\kappa$ -Opioid Receptor. *Biochemistry* **2009**, *48*, 6898–6908.
- (54) Polepally, P. R.; Huben, K.; Vardy, E.; Setola, V.; Mosier, P. D.; Roth, B. L.; Zjawiony, J. K. Michael Acceptor Approach to the Design of New Salvinorin A-based High Affinity Ligands for the Kappa-opioid Receptor. *Eur. J. Med. Chem.* **2014**, *85*, 818–829.
- (55) Roth, B. L.; Baner, K.; Westkaemper, R.; Siebert, D.; Rice, K. C.; Steinberg, S.; Ernsberger, P.; Rothman, R. B. Salvinorin A: a Potent Naturally Occurring Nonnitrogenous  $\kappa$  Opioid Selective Agonist. *Proc. Natl. Acad. Sci. U. S. A.* **2002**, *99*, 11934–11939.
- (56) Yan, F.; Mosier, P. D.; Westkaemper, R. B.; Stewart, J.; Zjawiony, J. K.; Vortherms, T. A.; Sheffler, D. J.; Roth, B. L. Identification of the Molecular Mechanisms by which the Diterpenoid Salvinorin A Binds to  $\kappa$ -opioid Receptors. *Biochemistry* **2005**, *44*, 8643–8651.
- (57) Lamb, K.; Tidgewell, K.; Simpson, D. S.; Bohn, L. M.; Prisinzano, T. E. Antinociceptive Effects of Herkinorin, a MOP Receptor Agonist Derived from Salvinorin A in the Formalin Test in Rats: New Concepts in Mu Opioid Receptor Pharmacology. *Drug Alcohol Depend.* **2012**, *121*, 181–188.
- (58) Wootten, D.; Christopoulos, A.; Sexton, P. M. Emerging Paradigms in GPCR Allostery: Implications for Drug Discovery. *Nat. Rev. Drug Discovery* **2013**, *12*, 630–44.
- (59) Spetea, M.; Asim, M. F.; Wolber, G.; Schmidhammer, H. The  $\mu$  Opioid Receptor and Ligands Acting at the  $\mu$  Opioid Receptor, as Therapeutics and Potential Therapeutics. *Curr. Pharm. Des.* **2013**, *19*, 7415–7434.
- (60) Vukojević, V.; Ming, Y.; D'Addario, C.; Hansen, M.; Langel, U.; Schulz, R.; Johansson, B.; Rigler, R.; Terenius, L. Mu-opioid Receptor Activation in Live Cells. *FASEB J.* **2008**, *22*, 3537–3548.
- (61) Langelier, B.; Linard, A.; Bordat, C.; Lavialle, M.; Heberden, C. Long Chain-polyunsaturated Fatty Acids Modulate Membrane Phospholipid Composition and Protein Localization in Lipid Rafts of Neural Stem Cell Cultures. *J. Cell. Biochem.* **2010**, *110*, 1356–1364.
- (62) Mahmood, I.; Liu, X.; Neya, S.; Hoshino, T. Influence of Lipid Composition on the Structural Stability of G-Protein Coupled Receptor. *Chem. Pharm. Bull.* **2013**, *61*, 426–437.
- (63) Saulière-Nzeh, A. N.; Millot, C.; Corbani, M.; Mazères, S.; Lopez, A.; Salomé, L. Agonist-selective Dynamic Compartmentalization of Human Mu Opioid Receptor as Revealed by Resolutive FRAP Analysis. *J. Biol. Chem.* **2010**, *285*, 14514–14520.
- (64) Guixà-González, R.; Ramírez-Anguita, J. M.; Kaczor, A. A.; Selent, J. Simulating G Protein-coupled Receptors in Native-like Membranes: From Monomers to Oligomers. *Methods Cell Biol.* **2013**, *117*, 63–90.
- (65) Ranganathan, A.; Dror, R. O.; Carlsson, J. Insights into the role of Asp79(2.50) in  $\beta 2$  adrenergic receptor activation from molecular dynamics simulations. *Biochemistry* **2014**, *53* (46), 7283–7296.
- (66) Granier, S.; Manglik, A.; Kruse, A. C.; Kobilka, T. S.; Thian, F. S.; Weis, W. I.; Kobilka, B. K. Structure of the  $\delta$ -opioid Receptor Bound to Naltrindole. *Nature* **2012**, *485*, 400–404.
- (67) Harding, W. W.; Tidgewell, K.; Byrd, N.; Cobb, H.; Dersch, C. M.; Butelman, E. R.; Rothman, R. B.; Prisinzano, T. E. Neoclerodane Diterpenes as a Novel Scaffold for  $\mu$  Opioid Receptor Ligands. *J. Med. Chem.* **2005**, *48*, 4765–4771.
- (68) Tidgewell, K.; Groer, C. E.; Harding, W. W.; Lozama, A.; Schmidt, M.; Marquam, A.; Hiemstra, J.; Partilla, J. S.; Dersch, C. M.; Rothman, R. B.; Bohn, L. M.; Prisinzano, T. E. Herkinorin Analogues with Differential Beta-arrestin-2 interactions. *J. Med. Chem.* **2008**, *51*, 2421–2431.
- (69) Collu, F.; Ceccarelli, M.; Ruggerone, P. Exploring Binding Properties of Agonists Interacting with a  $\delta$ -Opioid Receptor. *PLoS One* **2012**, *7*, e52633.
- (70) Riley, A. P.; Groer, C. E.; Young, D.; Ewald, A. W.; Kivell, B. M.; Prisinzano, T. E. Synthesis and  $\kappa$ -Opioid Receptor Activity of Furan-Substituted Salvinorin A Analogues. *J. Med. Chem.* **2014**, *57*, 10464–10475.
- (71) Standfuss, J.; Edwards, P. C.; D'Antona, A.; Fransen, M.; Xie, G.; Oprian, D. D.; Schertler, G. F. X. The Structural Basis of Agonist-induced Activation in Constitutively Active Rhodopsin. *Nature* **2011**, *471*, 656–660.
- (72) Li, J.; Edwards, P. C.; Burghammer, M.; Villa, C.; Schertler, G. F. Structure of Bovine Rhodopsin in a Trigonal Crystal Form. *J. Mol. Biol.* **2004**, *343*, 1409–1438.
- (73) Bailey, C. P.; Couch, D.; Johnson, E.; Griffiths, K.; Kelly, E.; Henderson, G. Mu-opioid Receptor Desensitization in Mature Rat Neurons: Lack of Interaction Between DAMGO and Morphine. *J. Neurosci.* **2003**, *23*, 10515–10520.
- (74) Saulière-Nzeh, A. N.; Millot, C.; Corbani, M.; Mazères, S.; Lopez, A.; Salomé, L. Agonist-selective Dynamic Compartmentalization of Human Mu Opioid Receptor as Revealed by Resolutive FRAP Analysis. *J. Biol. Chem.* **2010**, *285*, 14514–14520.
- (75) Xu, H.; Partilla, J. S.; Wang, X.; Rutherford, J. M.; Tidgewell, K.; Prisinzano, T. E.; Bohn, L. M.; Rothman, R. B. A Comparison of

Noninternalizing (Herkinorin) and Internalizing (DAMGO) Mu-opioid Agonists on Cellular Markers Related to Opioid Tolerance and Dependence. *Synapse* **2007**, *61*, 166–175.

## **Supporting Information**

### **Activation and Allosteric Modulation of Human $\mu$ Opioid Receptor in Molecular Dynamics**

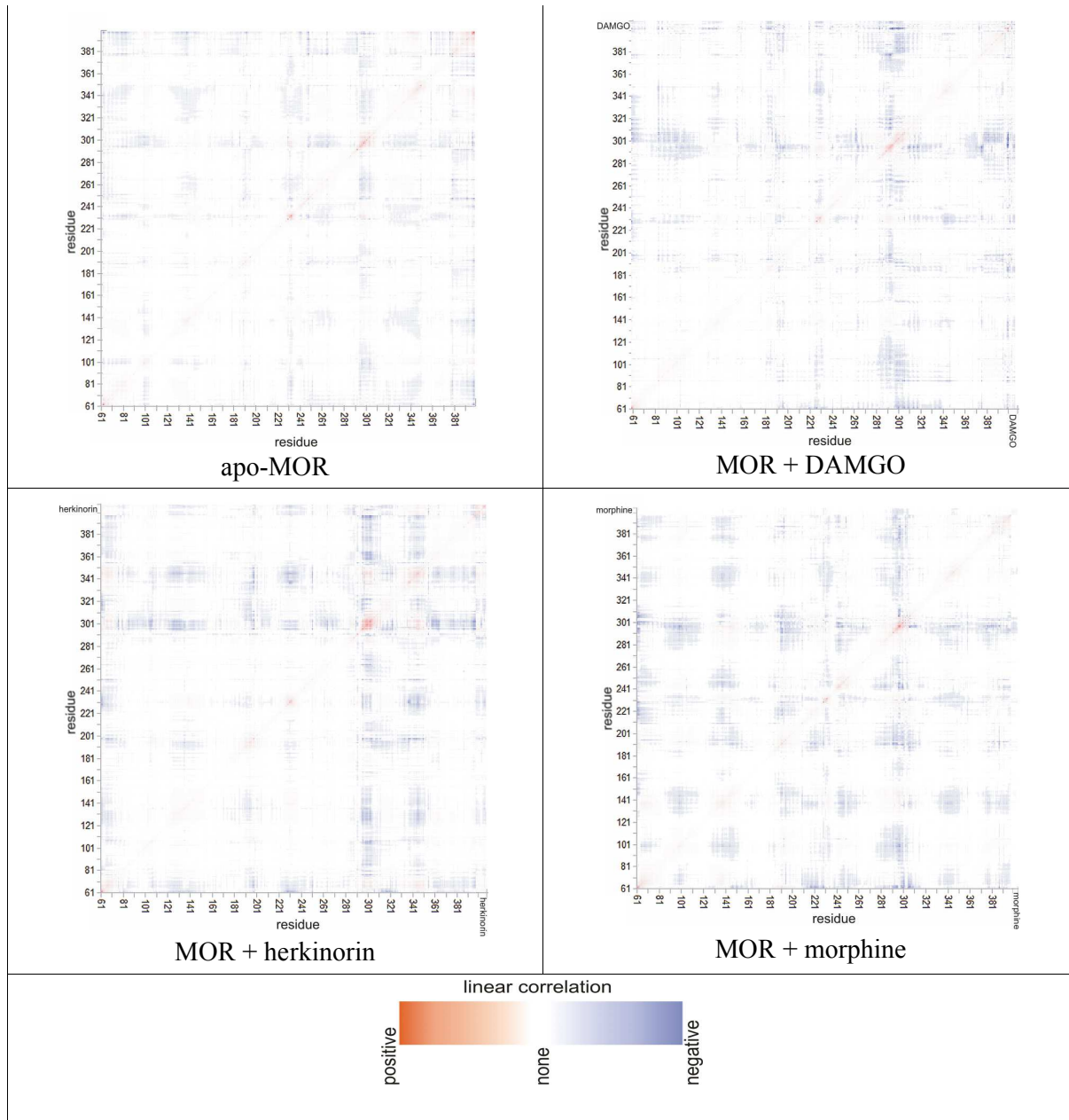
*Damian Bartuzi<sup>1</sup>, Agnieszka A. Kaczor<sup>1,2</sup>, Dariusz Matosiuk<sup>1</sup>*

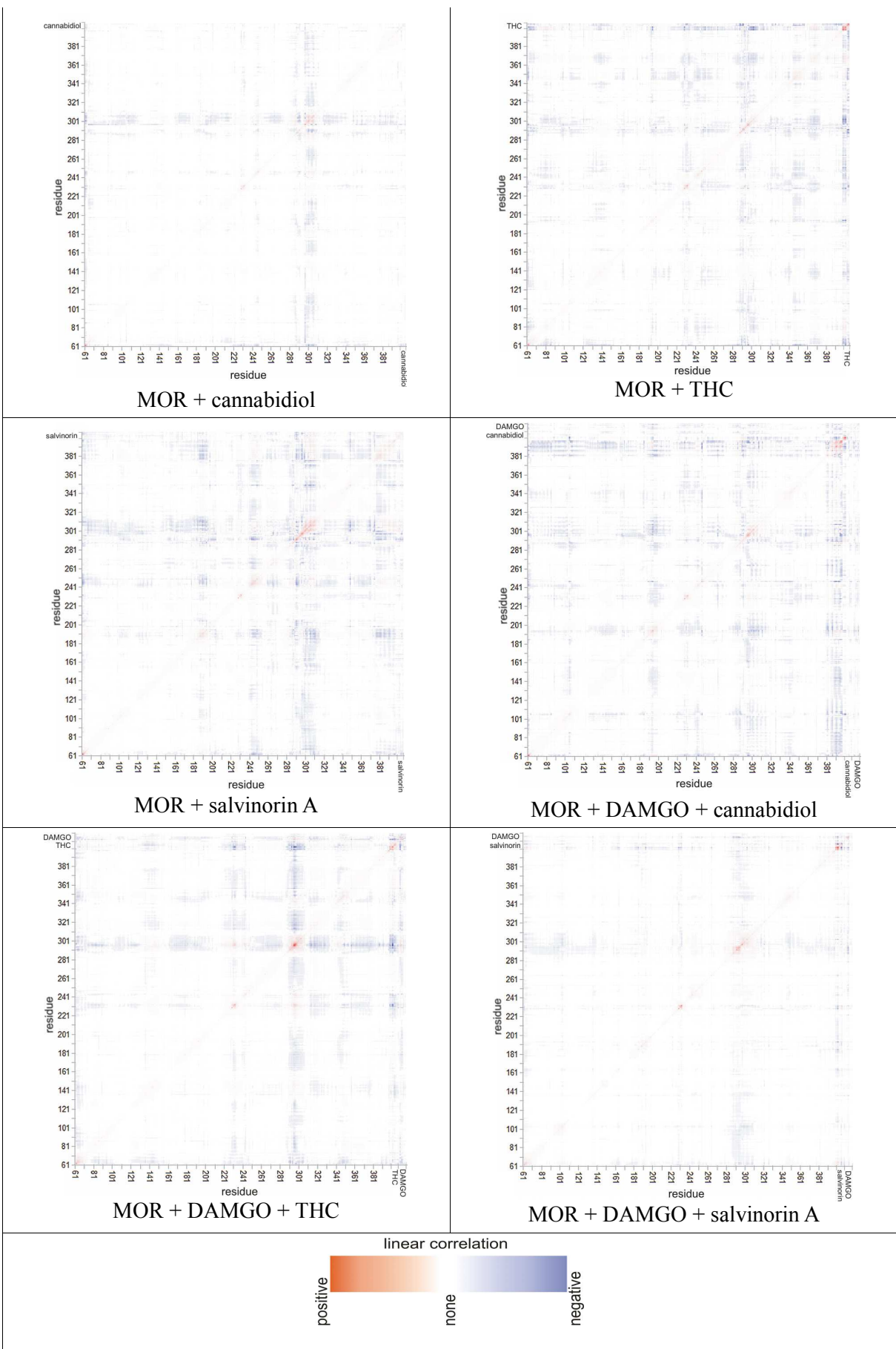
<sup>1</sup>Department of Synthesis and Chemical Technology of Pharmaceutical Substances with Computer Modeling Lab, Faculty of Pharmacy with Division of Medical Analytics, Medical University of Lublin, 4A Chodźki St., PL-20093 Lublin, Poland, tel.: +48815357365; fax: +48815357366

<sup>2</sup>School of Pharmacy, University of Eastern Finland, Yliopistonranta 1, P.O. Box 1627, FI-70211 Kuopio, Finland

e-mail: [damian.bartuzi@umlub.pl](mailto:damian.bartuzi@umlub.pl)

Table S1. Covariance matrices for simulations of  $\mu$  opioid receptor in complex with Gs protein with various ligands and allosteric modulators, performed in raft-like membrane. Modulator binding unharnesses linear correlations observed in agonist-bound receptor simulations, which is most pronounced in simulation of MOR+cannabidiol and MOR+DAMGO+Salvinorin A, but also evident in simulations MOR+THC, MOR+DAMGO+THC, MOR+DAMGO+cannabidiol.





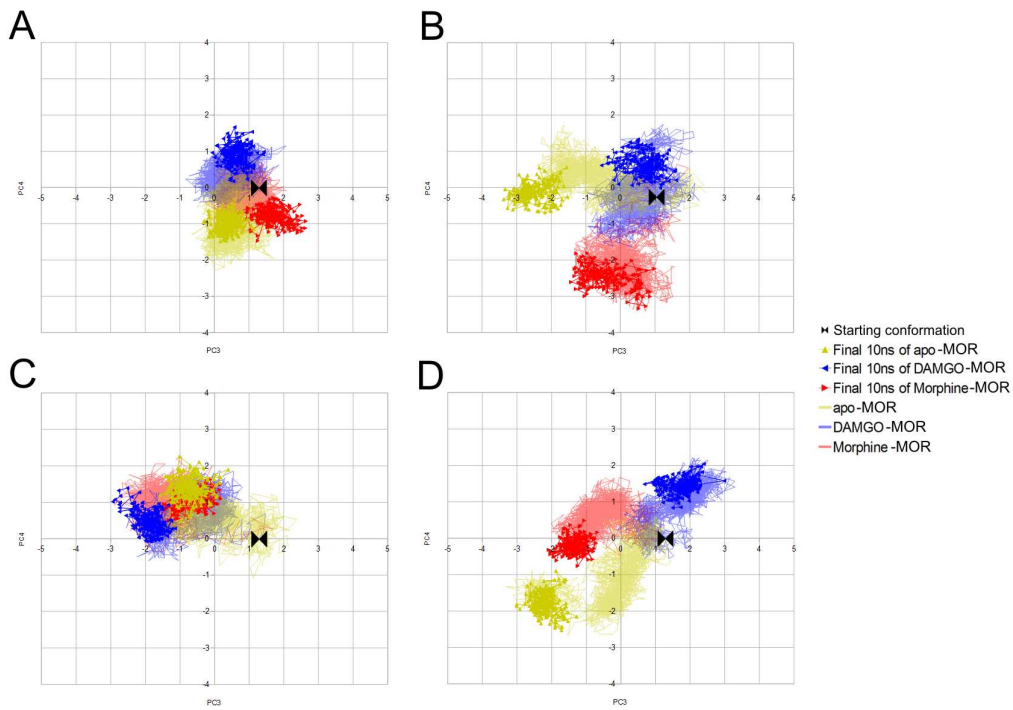


Figure S1. The third and the fourth principal components of morphine-MOR, DAMGO-MOR and the apo-MOR trajectories in four membranes in the common subspace. Plot presented in four parts for clarity. Main differences concern the pure POPC and 40% CHL membranes. A-raft-like membrane, B-POPC membrane, C- 20% CHL membrane, D – 40% CHL membrane.

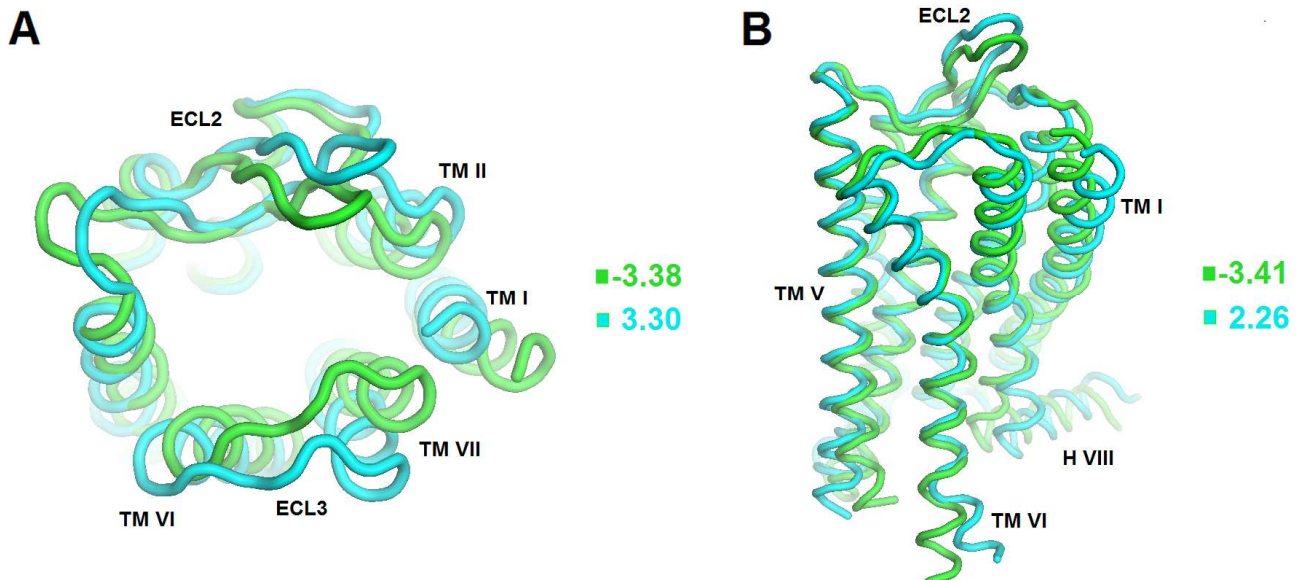


Figure S2. Trajectory projections on the average structure resulting from PCA of morphine-MOR, DAMGO-MOR and the apo-MOR trajectories in four membranes. Projections correspond to extreme values along the third (A) and the fourth (B) PC. The frames exaggerate occurring changes and do not show exact simulation snapshots. Legend corresponds to PC values from the Supplementary Figure 1. A – The PC3 contains mainly motions of the TM VII and the ECL2. B – The PC4 describes relative movement of the intracellular parts of TM V and TM VI, as well as some motions of the helix VIII and the ECL2.

Table S2. Averages and total drift of protein-modulator interaction energy values. Table refers to complexes in raft-like membrane.

Complex	Average Coulomb energy (kJ/mol)	Total Coul. Energy drift	Average VDW energy (kJ/mol)	Total VDW Energy drift
MOR+CDI	-33.08	5.26	-128.11	-4.06
MOR+THC	-17.55	3.93	-133.73	22.66
MOR+SAL	-30.91	17.32	-160.98	1.654
MOR+DAMGO+CDI	-38.12	-10.28	-120.87	-15.12
MOR+DAMGO+THC	-6.12	-4.07	-127.80	-19.05
MOR+DAMGO+SAL	-21.26	32.12	-135.90	55.41

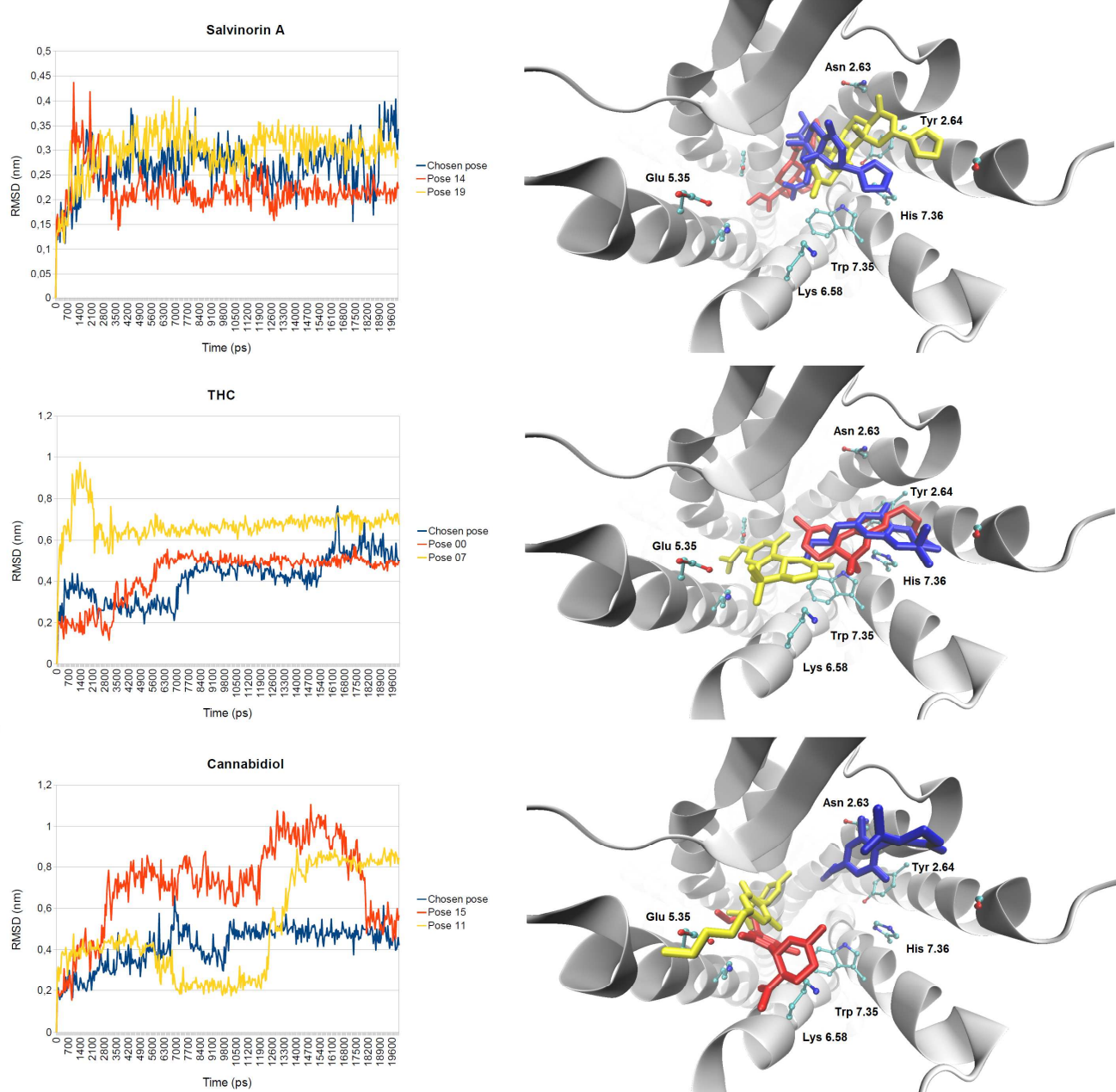


Figure S3. RMSD of the best docking poses of modulators during the initial 20 ns MD simulations.

Table S3. Number of different water molecules that occupied space within 5 Å from the conserved Asp 3.32 throughout simulations and their residence time. Table refers to complexes in raft-like membrane.

Ligands	DAMGO	DAMGO + CDI	DAMGO + THC	DAMGO + SAL
Very long-resident water molecules ( $t > 10$ ns)	9	9	17	21
Long-resident water molecules ( $10$ ns $> t > 1$ ns)	145	43	7	62
Medium-resident water molecules ( $100$ ps $< t < 1$ ns)	271	153	26	90
Short-resident water molecules ( $t < 100$ ps)	318	303	32	109
Total	743	508	82	282

Table S4. Number of different water molecules that occupied space within 5 Å from the conserved Asp 3.32 throughout simulations and their residence time. Table refers to complexes containing DAMGO and salvinorin A in different membranes.

Membrane	Raft-like		POPC		POPC + 20% CHL		POPC + 40% CHL	
Ligands	DAMGO	DAMGO+SAL	DAMGO	DAMGO+SAL	DAMGO	DAMGO+SAL	DAMGO	DAMGO+SAL
Very long-resident water molecules ( $t > 10$ ns)	9	21	2	5	6	8	12	4
Long-resident water molecules ( $10$ ns $> t > 1$ ns)	145	62	127	23	109	39	73	45
Medium-resident water molecules ( $100$ ps $< t < 1$ ns)	271	90	283	31	126	242	300	93
Short-resident water molecules ( $t < 100$ ps)	318	109	281	56	165	256	306	72
Total	743	508	693	115	406	498	691	214